

# Extreme sensitivity of the northeastern Gulf of Lion (western Mediterranean) to subsurface heatwaves: Physical processes and insights into effects on gorgonian populations~~devastating impacts on ecosystems~~ in the summer of 2022

Claude Estournel<sup>1</sup>, Tristan Estaque<sup>2</sup>, Caroline Ulses<sup>1</sup>, Quentin-Boris Barral<sup>1</sup>, Patrick Marsaleix<sup>1</sup>

<sup>1</sup>Université de Toulouse, LEGOS (CNES/CNRS/IRD/UT3), Toulouse, France

<sup>2</sup>Septentrion Environnement, Marseille, France

Correspondence to: Claude Estournel (claude.estournel@cnrs.fr)

**Abstract.** In the summer of 2022, ~~an~~-atmospheric ~~conditions situation~~ characterized by persistent anticyclonic anomaly caused an extreme marine heatwave in the western Mediterranean Sea. Time series of temperature profiles at various points along the northeastern coast of the Gulf of Lion (NW Mediterranean Sea) showed exceptional temperatures down to depths of 30 m ~~and which led to~~ massive mortality of benthic species. A hydrodynamic numerical simulation was used to analyze the physical processes responsible for this subsurface heatwave in a region where the climatology in summer is characterized by northerly winds inducing upwelling alternating with low winds. Firstly, the recurrence of heatwaves limited to the surface is demonstrated, triggered when upwelling stopped and warm water from the Northern Current intruded on the shelf. More importantly, in August and early September 2022, two episodes of southerly and easterly winds of 8 to 10 m·s<sup>-1</sup> occurred. The oceanic response to these winds was an alongshore cyclonic current advecting warm water onto the shelf and a downwelling of this warm water to depths of the order of 30 to 40 m. A large part of the Gulf of Lion coast was warmed by these events. However, the northeastern part of the shelf, on either side of the city of Marseille, was by far the area most affected in depth, due to the combination of the proximity of the warm surface waters of the Ligurian coast advected by wind-induced currents and the local acceleration of the wind by the continental topography, which intensifies the downwelling of these surface waters. These events are rare in summer, but their impact on the rich benthic ecosystems that characterize the region is dramatic, and will only increase with the warming trend in surface waters, already close to 1 °C for the last decade.

## 1 Introduction

With global warming, the number, intensity and duration of marine heatwaves (MHW) are on the rise, and MHW events occur throughout the year (Fox-Kemper et al., 2021). Impacts on marine organisms are likely to be most marked in coastal

28 areas. Benthic communities, being sedentary or having only limited mobility, are indeed particularly vulnerable to extreme  
29 temperatures (Lejeusne et al., 2010; Hughes et al., 2017; Garrabou et al., 2022) rather than to the exceedance of  
30 climatological values likely to occur throughout the year. This is the case for coral, for example, with a bleaching threshold  
31 defined for the Hawaiian Islands when surface temperature exceeds the maximum monthly mean by 1 degree (Glynn and  
32 D'Croz, 1990). When biological impacts are considered, it is therefore summer heatwaves that should be particularly  
33 monitored.

34

35 While surface MHW have been documented over several decades from satellite SSTs (Sea Surface Temperatures), in-situ  
36 data documenting temperatures in the first few tens of meters below the surface are infrequent, and their spatial  
37 representativeness varies greatly from site to site, particularly in coastal areas which are subject to unique dynamical  
38 processes due to the shallow depths and proximity to land (Schaeffer et al., 2023). On the one hand, irregularities in the  
39 coastline and submarine topography condition horizontal alongshore and cross-shore exchanges; on the other hand, spatial  
40 variations in the wind (possibly related potentially linked to continental relief) can generate localized coastal upwelling and  
41 downwelling depending on the orientation of the coastline relative to the wind direction. In contrast to upwelling, which  
42 counteracts the occurrence and intensity of heatwaves in the first few tens of meters of the water column (defined here as the  
43 sub-surface) and is identifiable on the SST, downwelling favors the penetration of warm surface water at depth, possibly  
44 beneath the stratified surface layer, and is generally not identifiable from the SST, especially as surface water can be cooled  
45 by air-sea heat fluxes (Schaeffer et al., 2023). Tracking coastal subsurface heatwaves is therefore impossible using surface  
46 information alone. As underlined by Schaeffer et al. (2023), the best proxy of sub-surface temperature extremes appears to  
47 be wind anomalies since sub-surface MHW events and years characterized by many sub-surface MHW days are  
48 predominantly associated with wind-driven downwelling. Numerical models are the only way to document them at high  
49 spatial (horizontal and vertical) and temporal resolution. However, their accuracy is a prerequisite when it comes to  
50 exceeding a tolerance threshold.

51

52 Since 1982, the Mediterranean SST has been warming at a mean rate of  $\sim 0.35$  °C/decade (Pastor et al., 2020), compared  
53 with the global mean increase of 0.15 °C/decade (Fox-Kemper et al., 2021). For the 2010-2019 decade, Garrabou et al.  
54 (2022) showed an increase in warming for an average of seven coastal sites in the north-western Mediterranean Sea, with  
55 values for the decade of 0.9 °C at 5 m and 0.6 °C at 35-40 m. Superimposed on this long-term warming, several authors  
56 have noted increased frequency, intensity and duration of MHW over the last four decades (Simon et al., 2022; Juza et al.,  
57 2022; Pastor et al., 2023) and an acceleration in recent years. Recently an exceptionally long-lasting and intense MHW,  
58 started in May 2022 (Martinez et al., 2023) and persisted until spring 2023 (Marullo et al., 2023). According to the latter  
59 authors, the intensity of this MHW was comparable to that of the 2003 event, which is the most intense case ever occurred in  
60 the last decades. The 2022 MHW was attributed to an atmospheric heatwave in Western Europe due to a persistent

61 anticyclonic anomaly (Guinaldo et al., 2023) exacerbated by climate change (Faranda et al., 2023). Never-before-recorded  
62 temperatures were observed at the surface of the western Mediterranean [Sea](#) during this summer (Guinaldo et al., 2023). In  
63 the Marseille area, east of the Gulf of Lion, temperatures exceeded 26 °C at 20 m for 4 days in August and 25 °C down to 30  
64 m for 3 days in early September (see more details in Grenier et al., 2022; Estaque et al., 2023). Following these last authors,  
65 depths from 25-30 m were exposed for the very first time to temperatures above 25 °C, considered as a potentially lethal  
66 acute heat stress threshold [for benthic species](#) (Crisci et al., 2011).

67

68 During the heatwaves of 1999 and 2003, large scale (>1000 km coastline) mass mortality events have affected numerous  
69 species of benthic invertebrates in the north-western Mediterranean [Sea](#) (Bensoussan et al., 2010 and references herein)  
70 indicating that they are living near their upper thermal thresholds. In the Parc National des Calanques south-east of  
71 Marseille, high temperatures in the summer of 2022 had an unprecedented impact on the mortality of numerous species,  
72 especially for the red gorgonian, *Paramuricea clavata*, and the red coral, *Corallium rubrum*, affecting depths down to 30 m  
73 (Estaque et al., 2023). Other emblematic species, such as sponges, have totally disappeared around Marseille at depths of  
74 down to 25 m, with only a few individuals surviving between 25 and 30 m (Grenier et al., 2022). The first sponge mortalities  
75 were recorded when temperatures exceeded 26 °C.

76

77 The aim of this article is to understand the interweaving of physical mechanisms from the large to the local scale at the origin  
78 of the summer 2022 [subsurface](#) heatwave, extreme in its intensity and impacts in the region of Marseille. To achieve this, we  
79 use numerical modeling checked against a dense network for top 40 m temperature measurement, called TMED-Net, which  
80 documents surface and subsurface heatwaves.

81

## 82 **2 Main characteristics of the study site**

83 The Gulf of Lion (Fig. 1) comprises a broad, crescent-shaped continental shelf enclosed between two straight coasts, the  
84 Ligurian coast to the northeast and the Catalan coast to the southwest, bordered by a narrow shelf and a steep continental  
85 slope, along which the Northern Current transports from northeast to southwest warm and low salinity waters [originating](#)  
86 from the south of the [western Mediterranean](#) basin and [ultimately originally](#) from the Atlantic. [Under certain meteorological](#)  
87 [conditions, the Northern Current splits into two branches, the coastal branch entering the continental shelf along the coast](#)  
88 [\(Barrier et al., 2016; Ross et al., 2016\). These intrusions occur particularly under stratified conditions.](#)

89

90

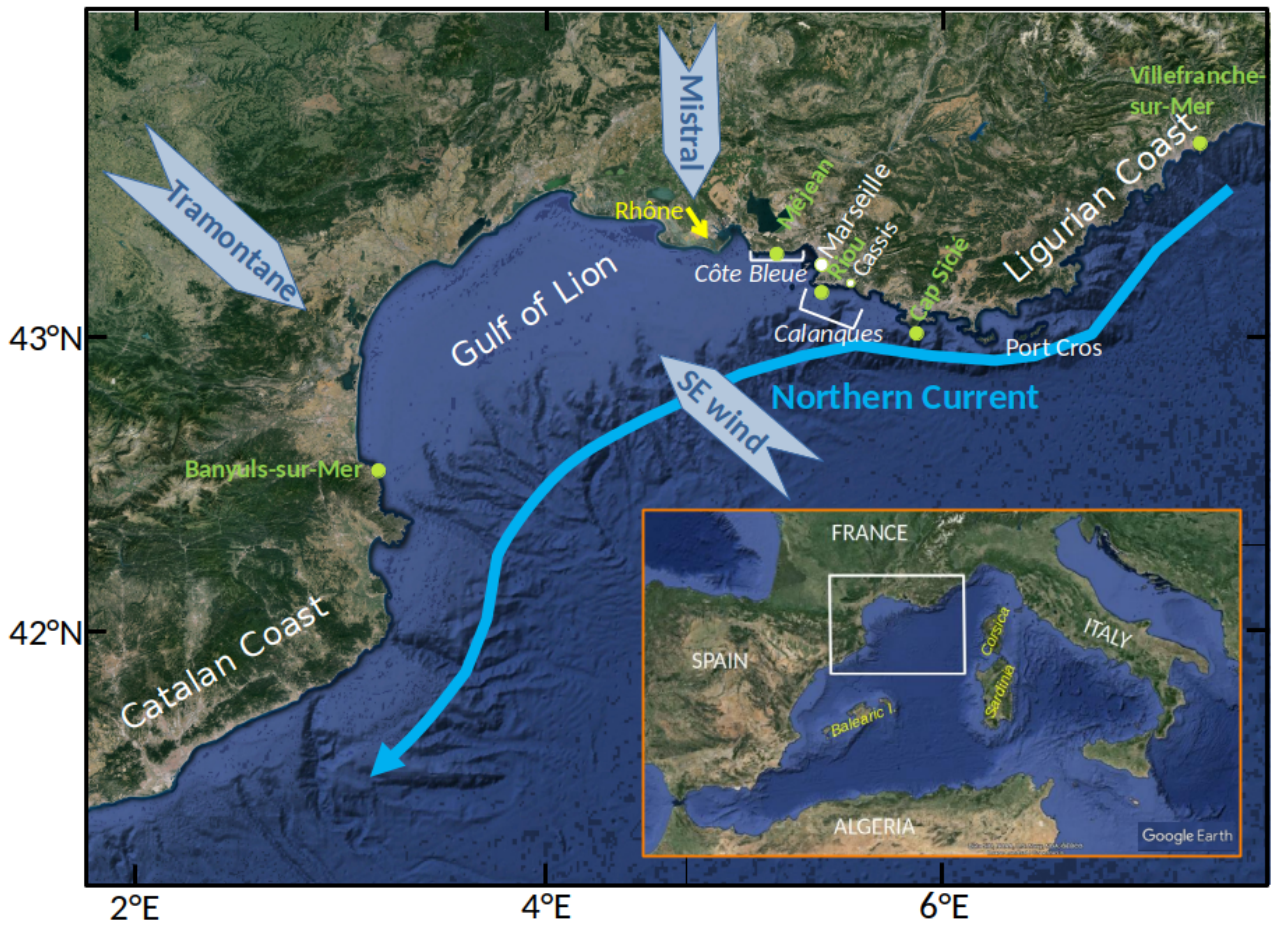


**Figure 1: Location and topography of the study area (background map from Google Earth). The prevailing Mistral and Tramontane winds, the southeast wind, the Northern Current, regional branch of the general circulation are indicated as well as the different places named in the text. The green solid circles indicate the TMED-Net observation points, Méjean, Banyuls-sur-Mer and Villefranche-sur-Mer on which comparisons with the model are focused, and Riou and Cap Sicié. The insert is a more general map of the western Mediterranean Sea, in which the area is indicated by a white rectangle.**

The north-western Mediterranean Sea is a mosaic of contrasting hydrological situations due to bathymetric constraints and complex wind regimes. In the Gulf of Lion, the prevailing winds blow from land (north to northwest, referred to in the following as the northerly winds for simplicity's sake) and are channeled by orography, the Rhone valley to the north, where the Mistral blows, and the passage between the Pyrenees and the Massif Central to the west, where the Tramontane blows. As a result, winds are much stronger in the Gulf of Lion than along the Catalan and Ligurian coasts. These northerly winds produce discontinuous coastal upwelling to the north of the zone, from around 3.5°E to 5.8°E (Millot, 1990), leading to surface cooling in summer that can exceed 10 °C in 1 to 2 days (Odic et al., 2022). Using criteria not detailed here, based on



the temperature anomaly with respect to climatology and the cooling between two successive days, the frequency of these events near Marseille between 2012 and 2022 averages 6.3 per summer (Barral pers. comm.). For ~~the same winds, (in this case, Tramontane)~~, the west coast is on the contrary favorable to downwelling (Bensoussan et al., 2010; Odic et al., 2022), producing less variable surface temperatures but nevertheless presenting lower maximum values than to the east (Paireud et al., 2014) due to ~~an increase in wind intensity and frequency from east to west the stronger and more frequent winds~~ (Obermann-Hellhund et al., 2018) and a reduced influence of the warm Northern Current.

110

~~After these northerly winds, the~~ second type of winds blows ~~across the western Mediterranean~~ from southwest to southeast, but locally these winds are strongly influenced by the relief of the islands and the mainland, which can strongly modify their intensity and direction. They generally enter the Gulf of Lion from a direction that varies from east after following the Ligurian coast, to southeast as they bypass Corsica and Sardinia, and to south. In what follows, we will refer to these winds as southeasterly winds in accordance with several authors (*e.g.* Millot, 1990; Odic et al., 2022). Rare in July-August, their frequency and intensity then increase sharply to peak in October-November (Odic et al., 2022), when it is frequently accompanied by precipitation on the mainland, which can lead to flash flooding of rivers, possibly accompanied by significant material and human damage (Ducrocq et al., 2014; Drobinski et al., 2014). These winds, which can reach  $25 \text{ m}\cdot\text{s}^{-1}$  in winter, induce cyclonic circulation around the Gulf of Lion, with currents of several tens of  $\text{cm}\cdot\text{s}^{-1}$ , accompanied by intensified downwelling to its southwestern tip due to the acceleration of currents linked to the narrowing of the continental shelf (Ulses et al., 2008; Mikolajczak et al., 2020).

122

The region around Marseille includes to the east the “Parc National des Calanques”, characterized by remarkable marine habitats (*e.g.* *Posidonia* meadows, coralligenous reefs, semi-dark caves, submarine canyons), 14 of which are considered rare and fragile (<https://www.calanques-parcnational.fr/en/marine-habitats>) and which presents a high risk of mass mortality associated to thermal stress for the red gorgonian (Paireud et al., 2014) as well as for other cnidarians, numerous sponge species, bryozoans and tunicates. To the west of Marseille, the “Parc Marin de la Côte Bleue” is another marine protected area, also hosting a great marine biodiversity similar to that found in the “Parc National des Calanques”, but at relatively shallower depths. In this last area, the presence of remarkable mesophotic ‘giant’ *Paramuricea clavata* forests is particularly noticeable (Sartoretto et al., 2023).

### 131 3 Material and Methods

We use a numerical simulation of the entire Mediterranean basin similar to that described in Estournel et al. (2021). The simulation is based on the 3D primitive equations SYMPHONIE model described in Marsaleix et al. (2008, 2006) and Damien et al. (2017), with turbulence closure and convection parameterization detailed in Estournel et al. (2016). The VQS (vanishing quasi-sigma) vertical coordinate (Estournel et al., 2021) is used with 60 levels. The horizontal resolution in the

136 area of interest is around 1900 m, which may seem coarse for an application very close to the coast, but [has](#) proved sufficient  
137 [to represent rapid temperature variations, as will be shown in section 4.1 devoted to simulation evaluation \(Fig. 2 and 3\).](#)  
138 ~~to achieve our objective.~~ The model [was](#) initialized and forced in the Gulf of Cadiz (Atlantic Ocean) from [daily](#) operational  
139 oceanic analysis produced by MERCATOR OCEAN International. ~~and a~~ At the surface [it was forced by](#) from the 12 hourly  
140 forecasts [that follow the 00.00 and 12.00 analyses](#) of the ECMWF operational meteorological model, ~~through~~ COARE bulk  
141 formulas ~~were~~ [used to compute](#) for the turbulent air/sea fluxes. The simulation was initialized in May 2011. Comparisons  
142 with monthly satellite SST taken at two seasons, 6 and 7 years after model initialization, show a very good representation of  
143 large-scale features present in the whole basin but also of various smaller structures (Estournel et al., 2021).

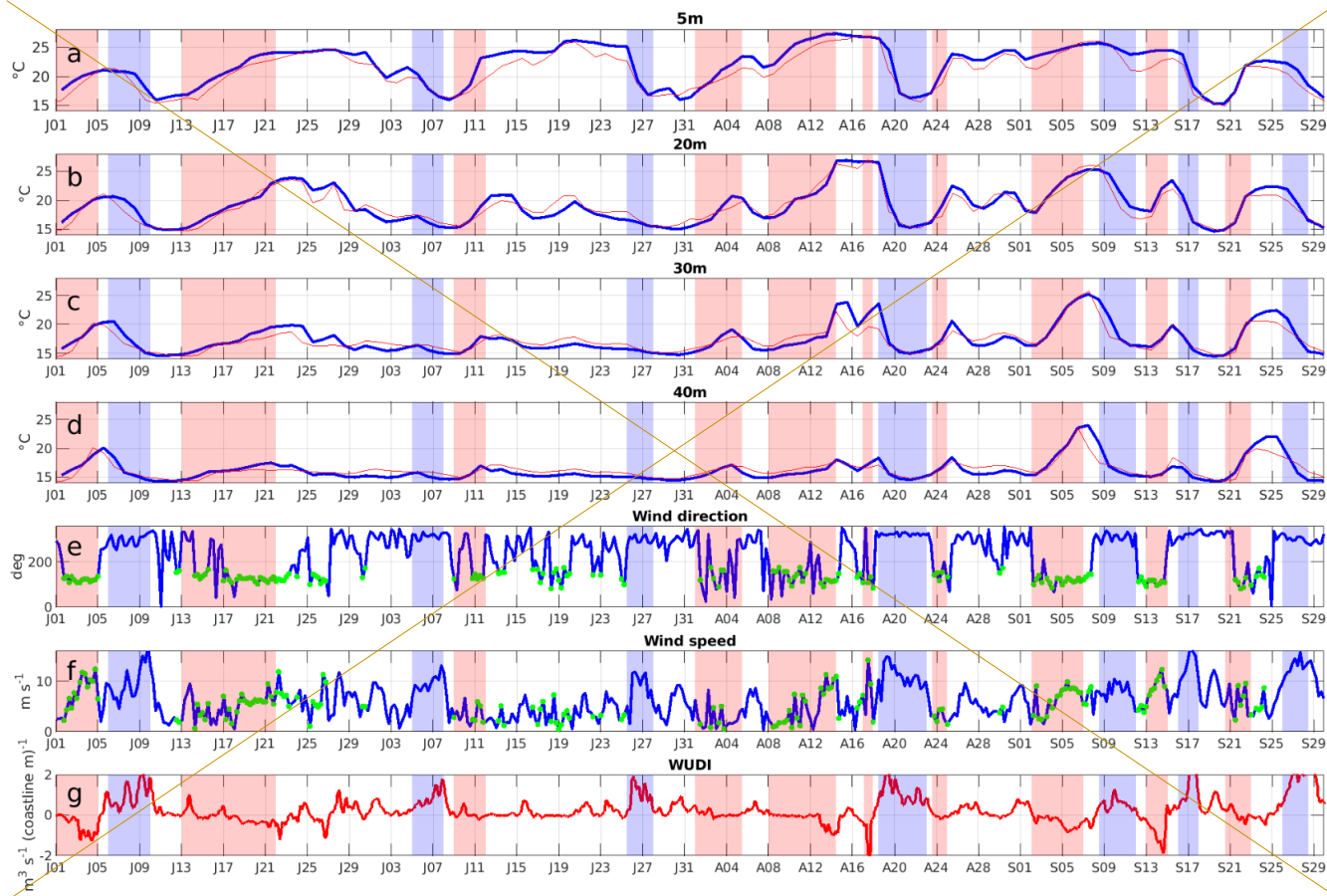
144  
145 At the coastal scale, the simulation is compared with TMED-Net (<https://t-mednet.org/>) observations taken at an hourly  
146 frequency every 5 m between 5 m and 40 m with autonomous sensors fixed to the seabed rocky substrate. ~~The summer of~~  
147 ~~2022 was marked around Marseille by mass mortality of sponges and gorgonians (see introduction).~~ This region includes  
148 various TMED-Net observation points stretching from the Côte Bleue to Cap Sicié. For our study, we focused on the Méjean  
149 site located 10 km west of Marseille (Fig. 1), where subsurface warming was generally strongest. We also took a broader  
150 view of the north-western Mediterranean [Sea](#), in order to visualize the specificity of the Marseille region. To do this, we  
151 compared temperature trends at Méjean with those recorded at TMED-Net points in Banyuls-sur-Mer and Villefranche-sur-  
152 Mer, located around 200 km to the south-west and north-east of Marseille (locations on Fig. 1). As mentioned in section 2,  
153 Banyuls-sur-Mer on the west coast of the Gulf of Lion is subject to frequent downwellings, and Villefranche-sur-Mer on the  
154 Ligurian coast is strongly impacted by the Northern Current.

155  
156 To link the intensity of the 2022 MHW with the extreme impacts observed on benthic communities to depths down to 30 m,  
157 we used a compiled dataset acquired by scientists and marine protected area managers in 2022, after the MHW. This dataset  
158 is the largest available for monitoring a mass mortality event for benthic organisms in the Mediterranean [Sea](#). The [in-situ](#)  
159 data was acquired using the methods detailed by Estaque et al. (2023), who analyzed some of the data in detail for the “Parc  
160 National des Calanques” area. Here, the dataset consists of [in-situ](#) data on the health of 18,465 colonies of red gorgonian (*P.*  
161 *clavata*), white gorgonian (*Eunicella singularis*) and yellow gorgonian (*Eunicella cavolini*), from 298 populations dwelling  
162 between the surface and 40 m depth. The data used allow us to compare the impact between the “Parc National des  
163 Calanques” (PnCal), the “Parc Marin de la Côte Bleue” (PMCB), the “Cap Sicié” (CS), and the “Parc National de Port-Cros”  
164 (PNPC), in relation to the differences in intensity of the 2022 MHW event.

166 **4.1 Assessment of the simulation and hydrological characteristics during summer 2022**

167 | ~~Figure-~~ A1 (Appendix A) shows the temporal evolution of measured and simulated temperature at Méjean between 5 and 40  
168 m and between 2012 and 2022. The simulation shows a cold bias of around 0.5°C at all levels, with uneven performance  
169 from year to year, particularly at 20 m depth, suggesting an uncertainty in the representation of the thermal gradient of the  
170 highly stratified layer beneath the surface mixed layer. The correlations between the observed and simulated series are above  
171 0.95. Rapid temperature variations in summer, reflecting the succession of upwelling and stratification events, are visible at  
172 all levels and are well synchronized, indirectly indicating a correct representation of wind in the simulation. The maximum  
173 of the series at 5 m is 27.8 °C in hourly values, reached in August 2022 (28.5 °C at Riou 20 km further south, sea location on  
174 Fig. 1). The duration of exceedance of the 25 °C value in 2022 is also the longest of the decade. The simulation agrees with  
175 observations on these two extremes of temperature and duration.

176  
177 Figures 2a to 2d zoom in on Fig. A1 from June to the end of September 2022. Correlations between observed and simulated  
178 | series range from 0.88 at 40 m to 0.96 at 5 m. The model bias is ~~maximum~~greatest at 5 m (-1 °C) and varies between -0.18  
179 and 0.15 °C at deeper levels. Warming episodes, highlighted in red, correspond to periods of continuous warming of at least  
180 5 °C either at the surface or at 20 m. Northerly winds inducing cooling episodes are highlighted in blue when they reach 10  
181 m·s<sup>-1</sup>.



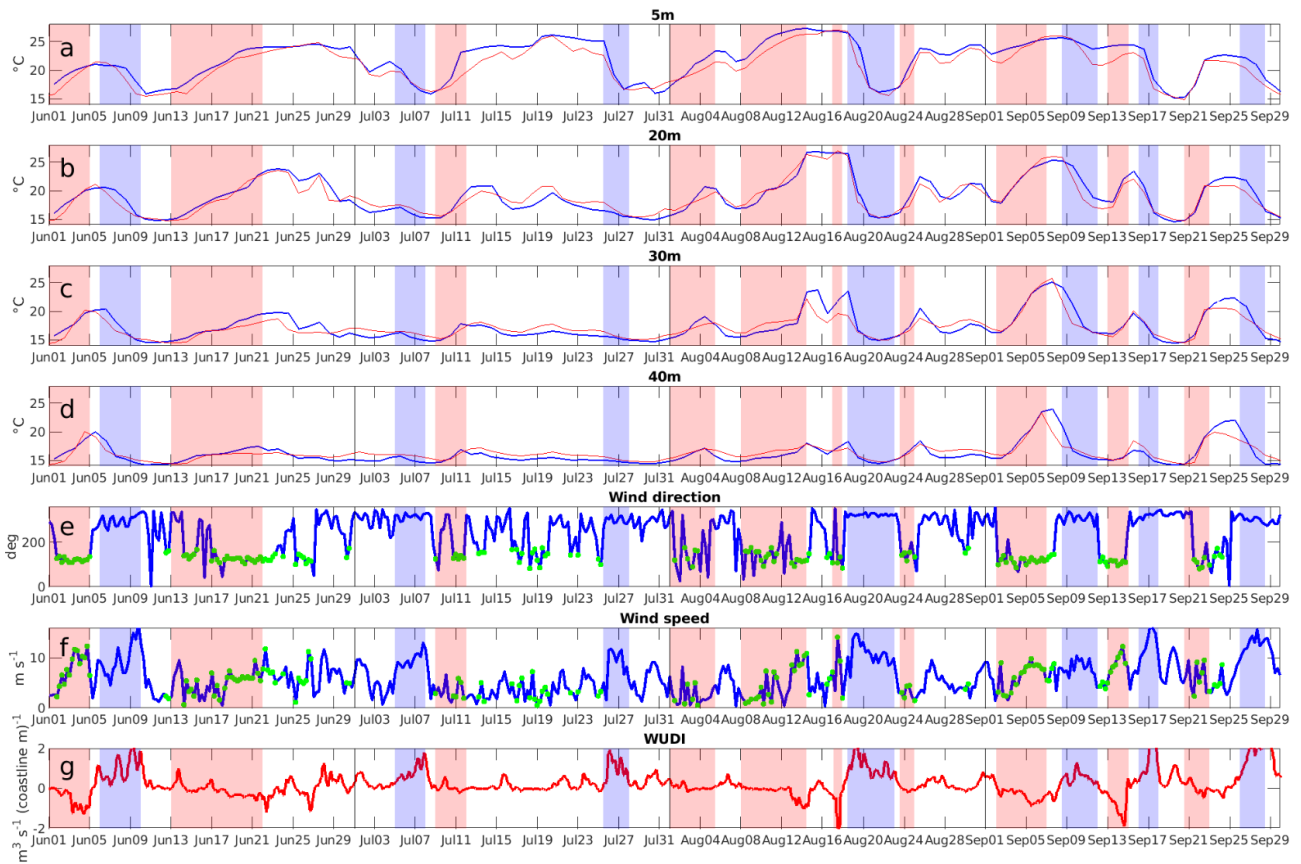


**Figure 2: Observed (blue) and simulated (red) daily averaged temperature time series at the Méjean point of the TMED-Net network during the summer of 2022 (June to September), from 5 m to 40 m, as indicated above the figures a-d. Wind direction and intensity (6-hour moving average) near Marseille, given by from the ECMWF operational-model (ocean model forcing) : (e and f). The southeasterly winds are indicated in green. Wind-induced Upwelling and Downwelling Index (6-hour moving average) calculated at Méjean (g). Warm events are highlighted by red stripes and northerly winds associated with cooling by blue stripes.**

Events above 25 °C at 5 m followed one another from July 19 to September 9, with contrasting signatures further down. The event that peaked at the surface on July 19 resulted in an increase of around 3 °C at 20 m, but was much less pronounced at greater depths. In contrast, the mid-August event was almost as warm at 20 m as at 5 m, with a signature at 30 m on August 14, shortly after the surface maximum, around +58 °C on August 14 compared to the beginning of the event, shortly after the surface maximum. The temperature during the early September event was almost uniform down to 30 m ( $T > 25$  °C) and reached 24 °C at 40 m.

Figure 3 compares the local characteristics of the subsurface heatwave observed by the TMED-Net network and simulated along the anticlockwise pathway of the Northern Current -at Villefranche-sur-Mer, Méjean, Banyuls-sur-Mer. In contrast to Méjean, Villefranche-sur-Mer's summer temperatures in 2022 did not vary greatly. The warm period extends over more than two months and generally involves a well-stratified surface layer. In Banyuls-sur-Mer, surface water temperatures are also

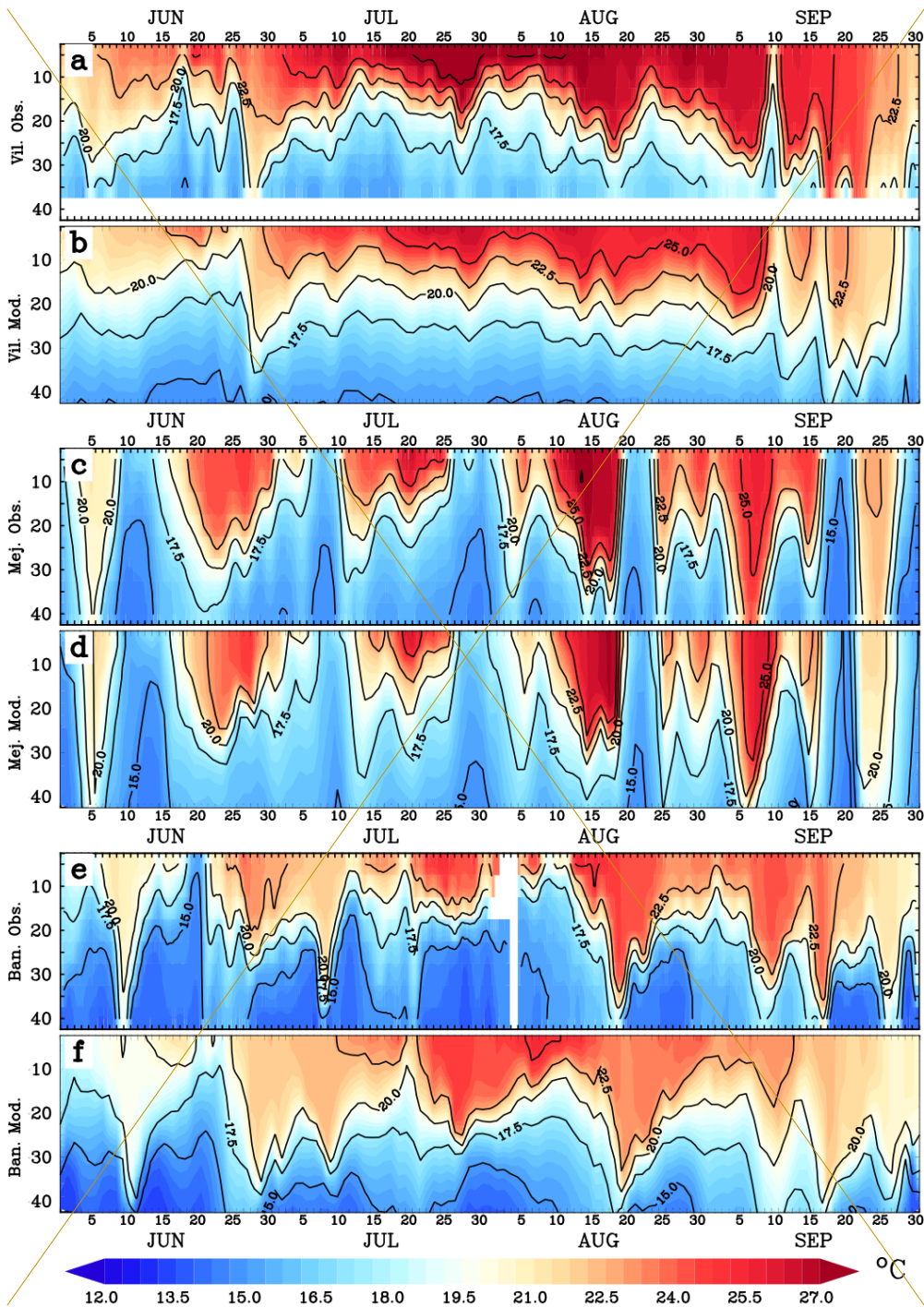


200 more continuous than in Méjean, but significantly lower than in Villefranche. On the other hand, the heat is distributed over  
201 a much thicker layer, evoking the recurrent presence of downwellings. The simulation reproduces the thermal regime at the  
202 various sites with shortcomings such as the underestimation of the surface layer temperature at Villefranche-sur-Mer.

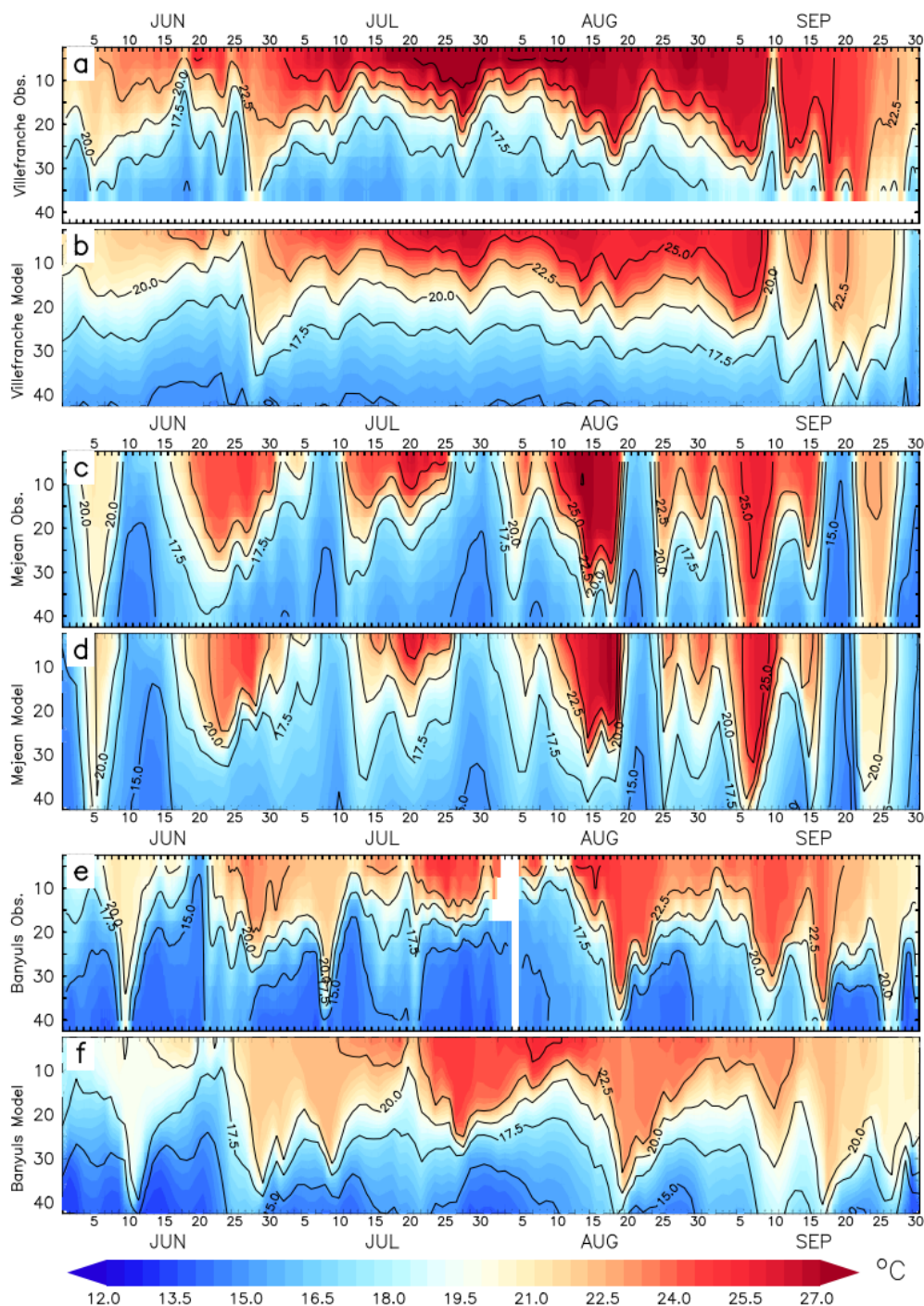
#### 203 4.2 Meteorological characteristics during summer 2022

204 | Figures 2 e,f show the wind direction and intensity of ECMWF ~~meteorological~~ model near Marseille. For greater visual  
205 clarity, hourly winds are averaged over 6 hours. Figure 2g illustrates the wind-induced upwelling and downwelling index  
206 (WUDI), as outlined by Odic et al. (2022), calculated with the ECMWF at the Méjean probe location. This index quantifies  
207 the horizontal Ekman transport within the model, exhibiting a positive ~~or (negative)~~ value, indicative of upwelling ~~(or~~  
208 downwelling, respectively). In line with climatology, the strongest winds blow from the mainland. Whenever the north,  
209 northwest wind exceeds  $10 \text{ m}\cdot\text{s}^{-1}$ , a surface temperature drop of at least  $5 \text{ }^{\circ}\text{C}$  is observed and simulated over the following  
210 days. This is the case for events starting on June 6, July 5 and 26, August 18, September 9, 16 and 26. These upwellings are  
211 also visible below the surface (especially if warming has taken place beforehand, as in the cases of June 6 and September 9).  
212 In this respect, it's worth noting that temperatures drop at depth around 24 hours before at the surface (see for example the  
213 June 6 event). In all of the aforementioned instances, the WUDI is greater than  $+0.5 \text{ m}^3\cdot\text{s}^{-1}\cdot(\text{coastline m})^{-1}$ , which is  
214 consistent with the previous identifications of upwelling.

215  
216 During summer 2022, warm events are characterized by lower wind intensities than northerly wind events. They are  
217 classified here as either weak winds (typically below  $5 \text{ m}\cdot\text{s}^{-1}$ ), or moderate southeasterly winds (typically above  $5 \text{ m}\cdot\text{s}^{-1}$  and  
218 rarely above  $10 \text{ m}\cdot\text{s}^{-1}$ ). All cases of weak or moderate southeasterly winds are indicated in green in Fig. 2 e,f and are all  
219 located in warm periods. Specifically, the periods in question are June 1-5, 13-22, July 9-12, August 1-4, 8-14, 23-25, and  
220 September 2-7, 13-15. For moderate wind speeds, the negative WUDI index below  $-0.5 \text{ m}^3\cdot\text{s}^{-1}\cdot(\text{coastline m})^{-1}$  suggests a  
221 potential contribution of downwellings to warming episodes.



222



223

224

225

226

**Figure 3: Hovmöller diagrams of the temperature (°C) profiles (m) given by the TMED-Net probes (a, c, e) and the model (b, d, f) at the locations of Villefranche-sur-Mer (a, b), Méjean (c, d) and Banyuls-sur-Mer (e, f) (see locations on Fig. 1). Isotherms every 2.5 °C. The probe diagrams are smoothed vertically and over 24 hours in order to facilitate optimal viewing.**

23

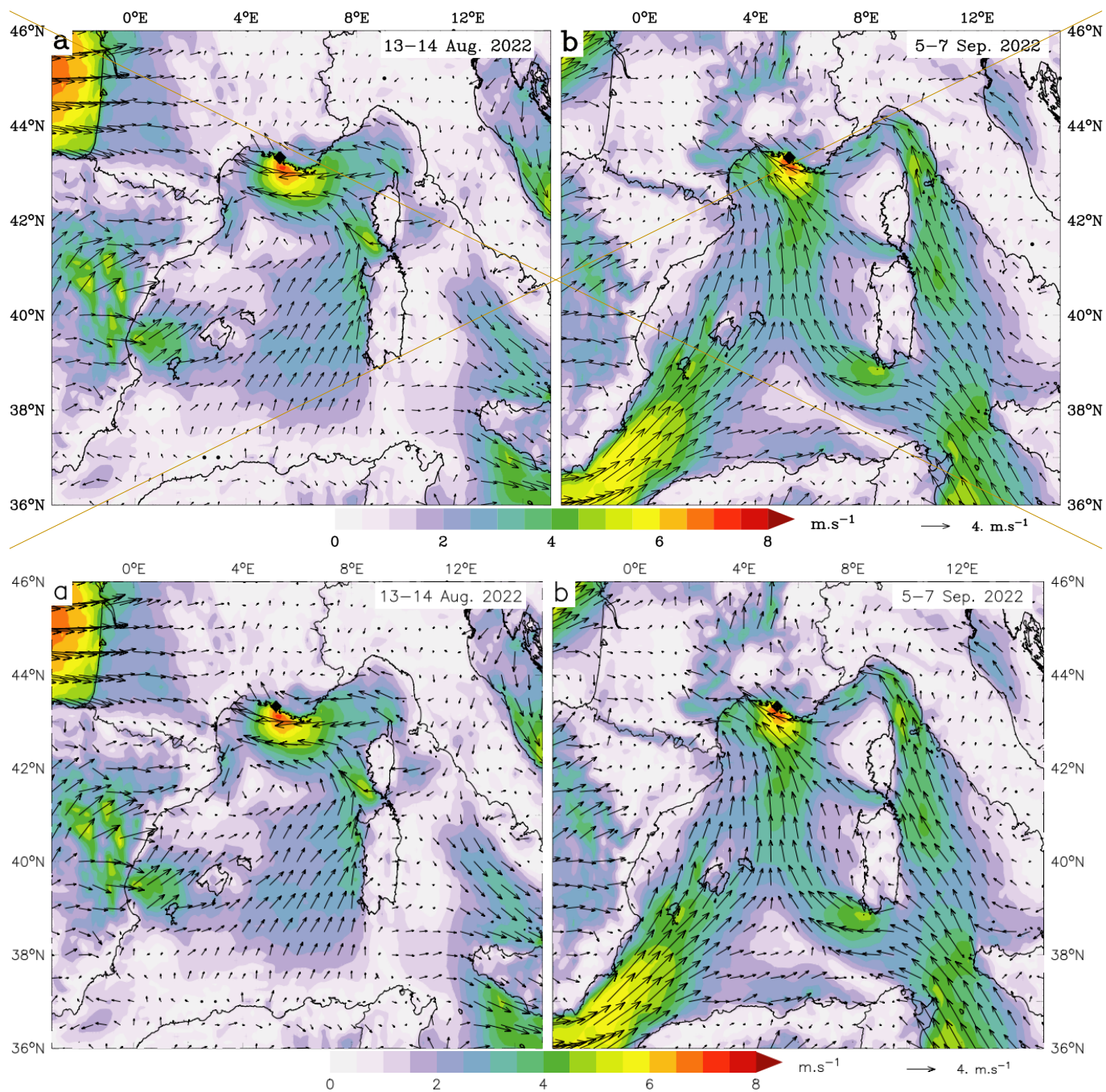
24

227 In order to characterize southeasterly winds over the summer of 2022 in relation to climatology, statistics have been  
228 compiled over the period 2012-2022. Each month, the time integral of negative WUDI (i.e. downwelling index) is  
229 calculated. Figure A2 (Appendix A) shows the climatology of this index, the dispersion over 11 years and the value for  
230 2022. Summer, and especially July and August, show very low values compared with autumn and winter, which also show  
231 very high interannual variability. For the summer of 2022, downwelling dynamics is particularly weak in July, while in  
232 August it is the strongest in the series, while remaining low compared to the rest of the year.

233  
234 Figure 4 shows the surface wind fields during the two warmest events at depth (30 m), on August 13-14 and September 5-7.  
235 In both cases, a low-pressure area was present over western Europe (western France in the first case, and the British Isles in  
236 the second) leading to a southerly flow over the Mediterranean Sea, which penetrated the mainland in the Gulf of Lion. This  
237 flow in the lower layers of the atmosphere was strongly influenced and accelerated by the relief especially by Corsica and  
238 Sardinia, which were bypassed by veins of wind between and around the two islands. These wind veins converged in the  
239 eastern Gulf of Lion, here influenced by the topography of the Provençal coast and the edge of the Alpine chain, producing a  
240 noticeable acceleration in the vicinity of Marseille.



241



242

243

244

**Figure 4: ECMWF  $\mathbf{W}_{\text{wind}}$  field ( $\text{m}\cdot\text{s}^{-1}$ ) at 10 m averaged over the two warmest subsurface periods: (a) 13-14 August 2022 ; (b) 5-7 September 2022. The black diamond stands for the Méjean observation point.**



## 245 4.3 Marine heatwaves

246 The warmest event at the surface and at 20 m ~~at Méjean, that triggered sponge mortality,~~ occurred in mid-August. At 30 and  
247 40 m, temperatures peaked later in the season, during the September 6 event. Events were longest at the surface: the major  
248 event in mid-August lasted around 2 weeks. While warm events were characterized by weak wind or moderate southeasterly  
249 wind conditions, they were stopped by northerly wind gusts along the northern coast (Fig. 2). The points discussed in the  
250 following 3 subsections are: warming during weak wind conditions (4.34.1), ~~and and~~ during moderate southeasterly winds  
251 (4.34.2), and sensitivity of sub-surface warming to the duration of southeasterly winds (4.34.3). ~~From mid-August onwards,~~  
252 ~~impacts appeared as massive mortalities down to 25 m, and more moderately at 30 m. A sensitivity study will explore the~~  
253 ~~temperature response to an extension of the wind period.~~

### 254 4.3.1 Case of weak winds: Impact of pre-existing upwelling

255 The upwellings that characterize the region studied here are mechanisms that a priori protect the coast from MHW by  
256 renewing surface water with deep cold water. However, Barrier et al. (2016) have highlighted a collateral effect that occurs  
257 when the upwelling stops, in the form of intrusions of the Northern Current on the Gulf of Lion shelf with a delay of 1 day  
258 after the wind relaxation. The impact of these intrusions on the occurrence of heatwaves in the eastern Gulf of Lion is  
259 described in this section.

260  
261 Five warming episodes were considered: June 13-18, July 9-12, August 1-4, August 8-12 and August 23-25, characterized  
262 by winds of less than  $5 \text{ m}\cdot\text{s}^{-1}$ , mostly blowing from the southeast, with occasional short spells from the northwest (Fig. 2).  
263 For each of these events, the temperature rise at 5 m ~~ranged from~~ increased by 4 to  $7^\circ\text{C}$  (on average  $5.4^\circ\text{C}$ ). At 20 m, the  
264 warming was slightly lower (~~averaging~~  $5^\circ\text{C}$  on average), ~~then and It continued~~ continue to decrease ~~decreased~~ at 30 m ~~to an~~  
265 ~~average value of~~ ( $3^\circ\text{C}$  on average) and at 40 m ~~to~~ ( $1.9^\circ\text{C}$  on average) (more details on the different events in Table A1 in  
266 Appendix A). ~~While the warming at depth could be attributed to downwelling, this cannot be the case~~ The warming at 5 m  
267 ~~;cannot be due to a downwelling~~ -as this would imply a considerable temperature gradient between the surface and 5 m.  
268 Let's now consider the role of the solar radiation to explain this warming. ~~ease of~~ For the July 9-12 event, ~~for which~~ the  
269 warming at 5 m was  $6.7^\circ\text{C}$  ~~in two days~~ and  $5.4^\circ\text{C}$  at 20 m, in two days. The warming induced by the absorption of the heat  
270 associated to solar radiation, equal to  $320 \text{ W m}^{-2}$  on average over 24h, is around  $0.8^\circ\text{C}$ . ~~Net solar radiation at the surface~~  
271 ~~averaged over 24 hours was  $320 \text{ W m}^{-2}$ . If we consider that this flux was absorbed by a 20 m thick layer, the warming~~  
272 ~~resulting from this absorption over 2 days would be  $0.8^\circ\text{C}$ , i.e. much lower than observed, which rules out the hypothesis of~~  
273 ~~warming by the atmosphere (the solar flux in this case). Warming is therefore almost caused by a mechanism internal to the~~  
274 ocean. For each event considered, the warming at Méjean started between 1 and 3 days after the end of a northerly gale  
275 (varying in intensity from  $8$  to  $15 \text{ m}\cdot\text{s}^{-1}$ ) and of the associated upwelling, which fits perfectly with the observations of Barrier  
276 et al. (2016) cited above. ~~In such conditions of northerly wind cessation during stratified periods, Barrier et al. (2016) have~~

277 | highlighted intrusions of the Northern Current on the Gulf of Lion shelf with a delay of 1 day after the wind relaxation. This  
278 | process is ~~therefore~~ responsible for the observed warming. The processes associated with upwelling relaxation explain the  
279 | ~~observed and simulated surface warming, which, in our case, and but it~~ implies that the water mass advected ~~during~~ by the  
280 | Northern Current intrusion was much warmer than that present on the Gulf of Lion prior to the upwelling. The eastern part of  
281 | the Gulf of Lion is particularly favorable to this situation, as it borders to the east of 6°E, an area much less exposed to  
282 | northerly winds and therefore much more continuously warmer at the surface (see the times series at Villefranche sur Mer in  
283 | Fig. 3a).

284 |  
285 | As an example, Fig. 5 a,b,c show the surface temperature and current for the second warming episode, on July 8, 12 and 15:  
286 | at the peak of the northerly wind and upwelling on July 8, during and at the end of the warming phase on July 12 and 15,  
287 | respectively. The intrusion of a branch of the Northern Current ~~producing the renewal of surface water by the~~ advecting on of  
288 | warm water is visible along the coast in the Marseille area after the stop of the northerly wind: ~~t~~ The advected warm water  
289 | mass was located east of 6°E on July 8 (Fig. 5a), then 50 km further west on July 12 (Fig. 5b) and around 100 km (up to 5°E)  
290 | on July 15. (Fig. 5c). It is also interesting to note that the strong, sustained northerly wind ( $\sim 10 \text{ m}\cdot\text{s}^{-1}$  for 4 days) which  
291 | preceded the warming episode, produced marked hydrological structures (Fig. 5a) such as the upwelling front stretching  
292 | southwards off Marseille and, further west, organized cross-shore currents. These structures, which persist for a few days,  
293 | ~~seem to probably~~ hinder the westward progress of warm waters ~~westwards~~.

294 |

#### 295 | 4.3.2 Case of moderate to strong southeasterly winds

296 | Odic et al. (2022) showed the tight correlations between downwelling favorable winds and 35 m temperature anomalies  
297 | along the nNorth-western Mediterranean shorelines. They quantified that the 75th percentile of the WUDI index for  
298 | downwelling corresponded to an alongshore wind close to  $5 \text{ m}\cdot\text{s}^{-1}$  and a temperature response of  $+3^\circ\text{C}$  at 35 m for stratified  
299 | conditions. Here, we examine the impact of such downwelling on subsurface heatwaves. According to Juza et al. (2022) and  
300 | Darmaraki et al. (2024), such downwelling processes may indeed facilitate the vertical extension of heatwaves in the western  
301 | Aegean and northeastern Crete.

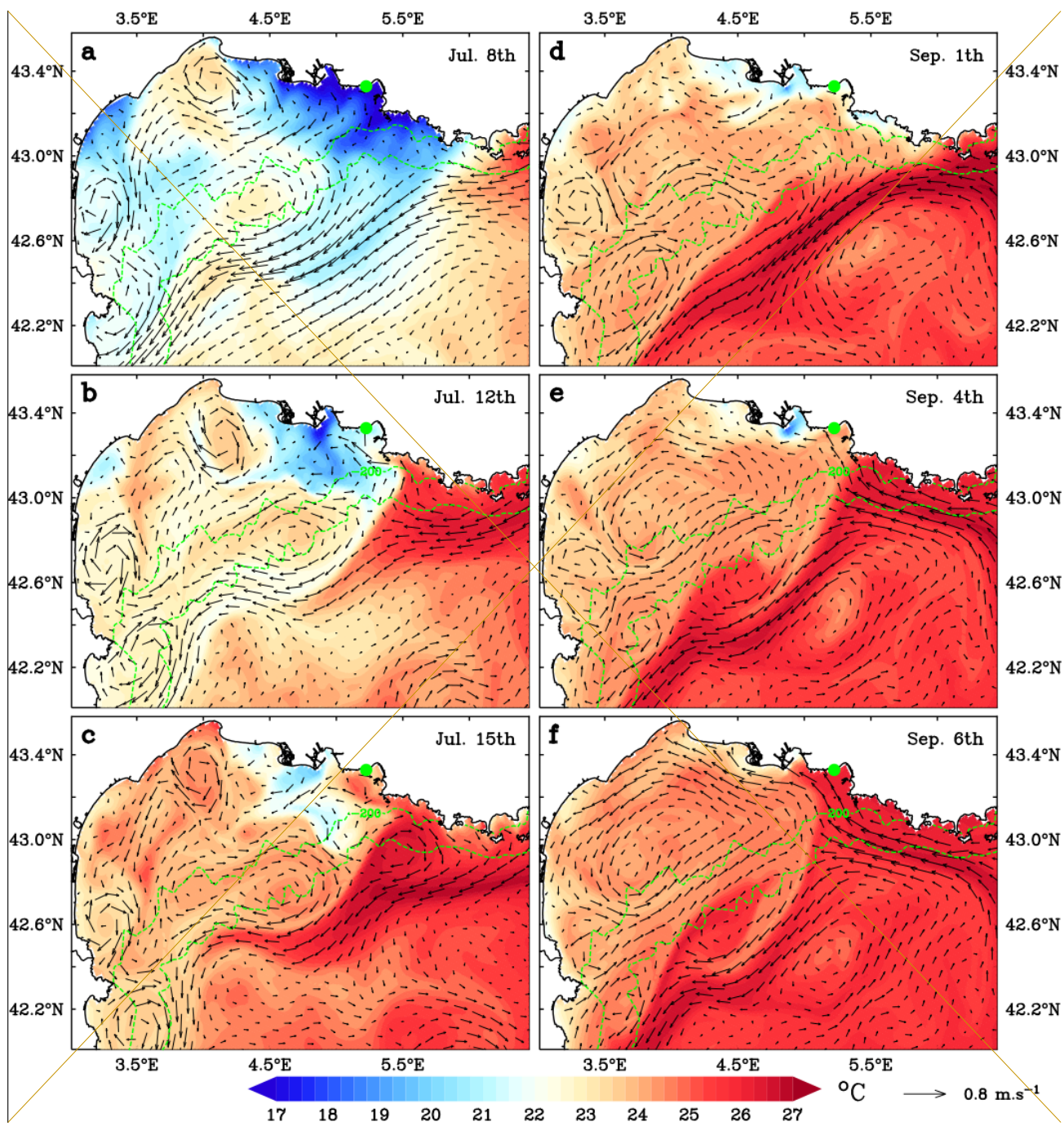
302 |

303 | We consider here the two cases associated with the warmest temperatures at 20 m: ~~the second part of the major August~~  
304 | ~~event, from~~ August 12 to 14 event extended by a secondary new peak on the 17th, and ~~the period from the~~ September 2 to 7  
305 | event. In both cases, the southeasterly wind ~~whose average is~~ presented in Fig. 4, exceeded  $8 \text{ m}\cdot\text{s}^{-1}$  and the WUDI index fell,  
306 | showing coastward transports of over  $0.5 \text{ m}^3\cdot\text{s}^{-1}\cdot(\text{coastline m})^{-1}$  that lasted 2 days (Fig. 2). The vertical distribution of  
307 | warming was quite different from that of low winds (Fig. 2, Table A1 & Fig. 3) : In contrast to the low-wind cases, warming  
308 | was minimal at the surface, as temperatures were already high at the start of both events. In terms of the vertical extension  
309 | of warming, the difference with low-wind cases is striking (Fig. 2, Table A1 & Fig. 3). Warming and increased down to 30

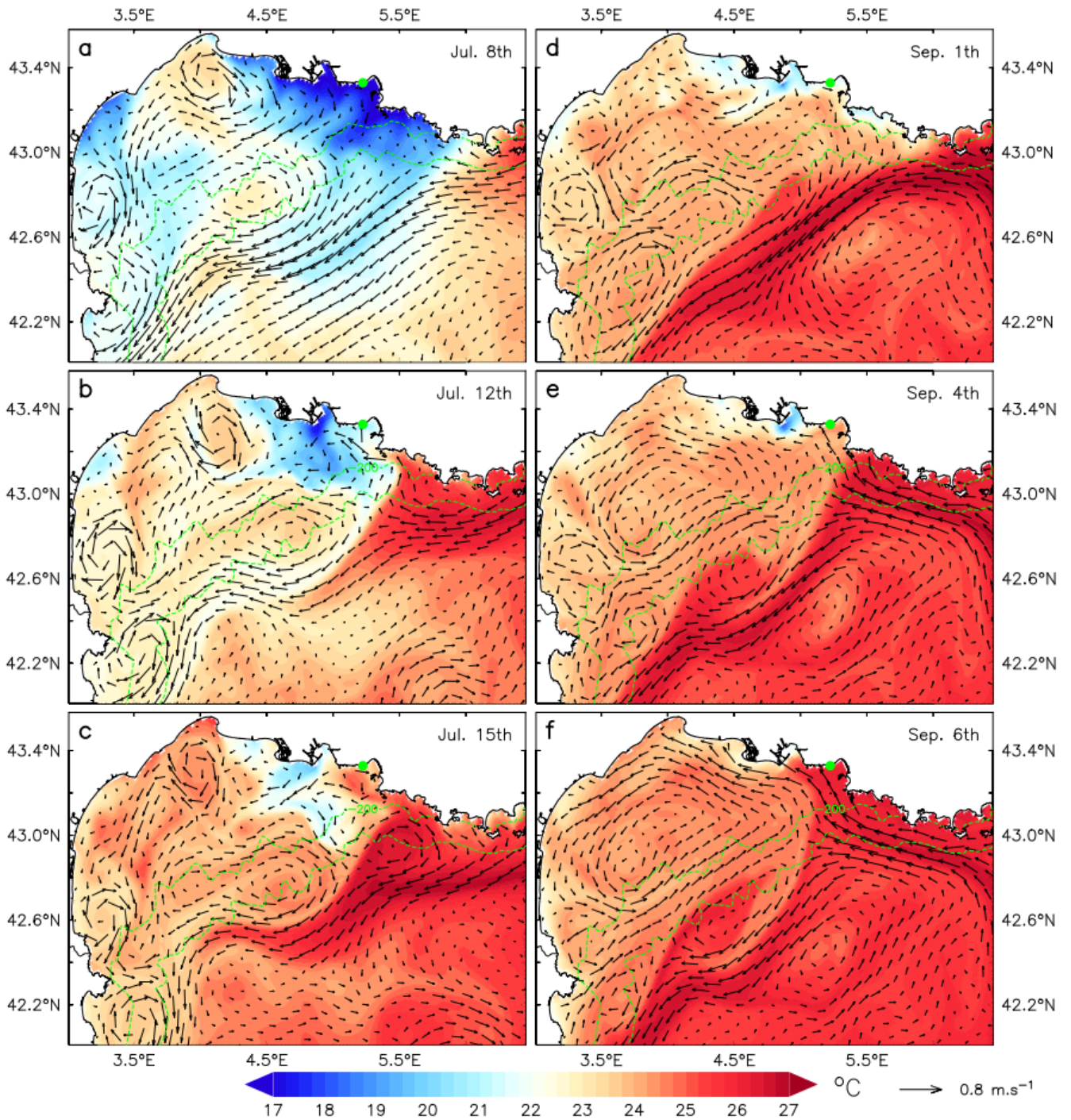
31  
32

310 m, with values of 5.5 °C in August and 8.8 °C in September (compared with 2-3.6 °C for weak winds). ~~At 40 m, For the first~~  
311 ~~event, for which the southeasterly wind is of shorter duration,~~ warming ~~was~~ 2 °C ~~for the first (and shorter) event at 40 m,~~ and  
312 8.5 °C for the second one. Again in contrast to the low-wind cases, the northerly wind preceding the September 6 event was  
313 weak (less than 10 m·s<sup>-1</sup>) and of short duration (from August 31 to September 1): ~~and As~~ as a result, the associated upwelling  
314 (Fig. 5d) and the currents on the inner shelf were poorly developed, ~~as can be seen from the comparison with Fig. 5a~~ We  
315 ~~cannot~~ ~~t~~ and ~~the expect a massive~~ intrusion of the Northern Current ~~and significant warming~~ associated with the cessation of  
316 upwelling ~~was weak~~. ~~In this case,~~ The warming during this event was therefore rather ~~related~~ due to the southeasterly wind  
317 causing surface water to pile up against the coast, inducing the downwelling of warm surface water, and finally, through  
318 geostrophy, the development of an alongshore westward jet. The persistence of the easterly wind (6 days without  
319 interruption) and the weak currents that prevailed before ~~the easterly wind~~, favored the establishment of this alongshore  
320 circulation at the whole continental shelf scale, warming a large part of the coastal zone of the Gulf of Lion between  
321 September 1 and 6, as shown in Fig. 5f. At a depth of 30 m, Fig. 6a-c show the pre-event and peak temperatures and their  
322 differences, indicating that the eastern Gulf of Lion was considerably warmed up by around 7°C over 600 km<sup>2</sup> from 5.62°E  
323 east of Cassis to 4.85°E near the Rhône mouth. Further west, the coastal strip extending up to the 60 m isobath was heated by  
324 2 to 4 °C. The similarity between the area of maximum warming and that of maximum downwelling favorable winds (Fig.  
325 4b) is remarkable.

326

35  
36

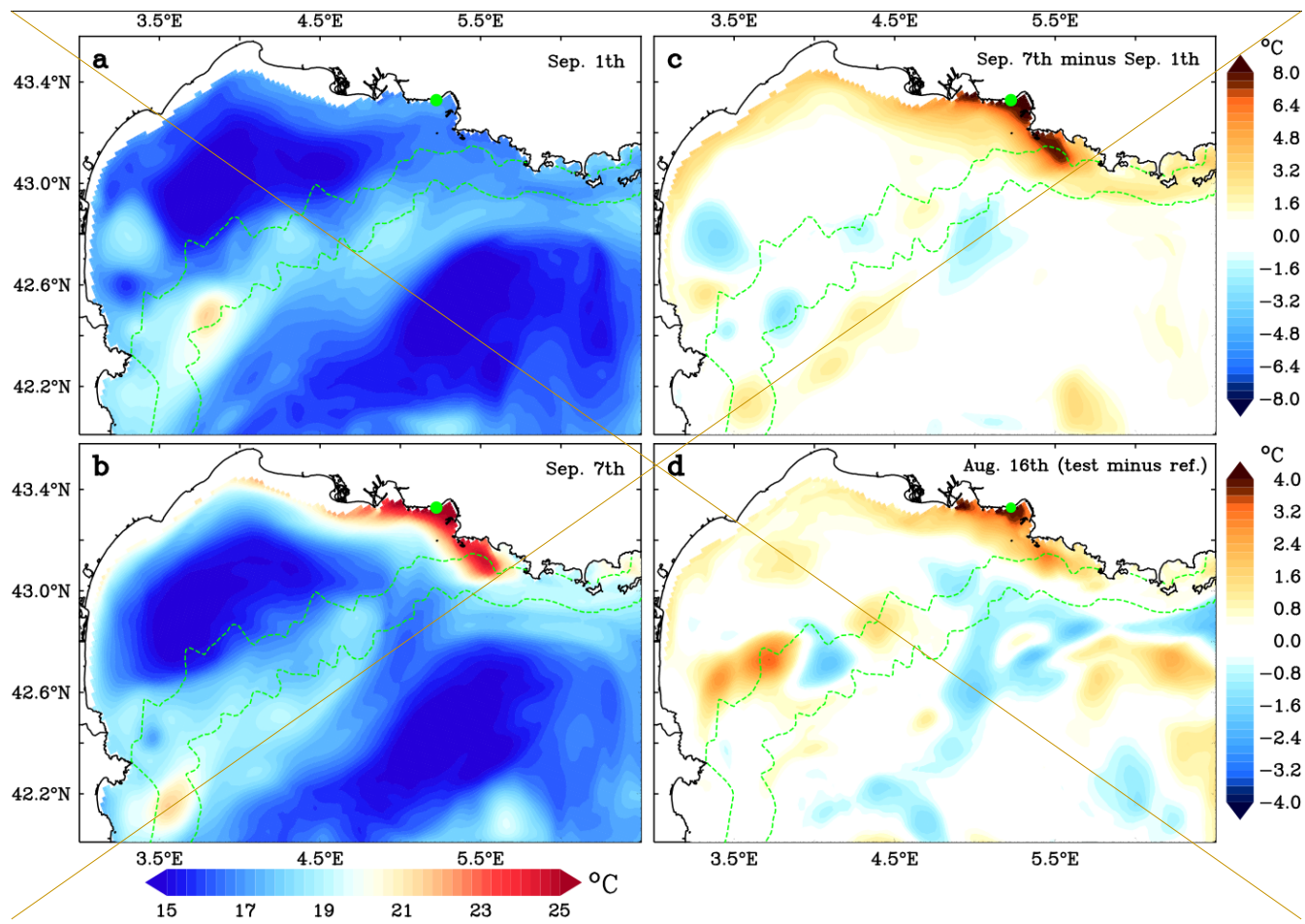




**Figure 5: Surface temperature (°C) and current simulated for the surface warming event of July (a,b,c) : (a) July 8 (during the upwelling), (b) July 12 (the day after the wind stopped), (c) July 15. Same for the subsurface warming event of September (d,e,f): (d) September 1, (e) September 4, (f) September 6. The green point stands for the Méjean TMED-Net observation point. The green dashed lines are the 200 and 1000 m isobaths.**



332



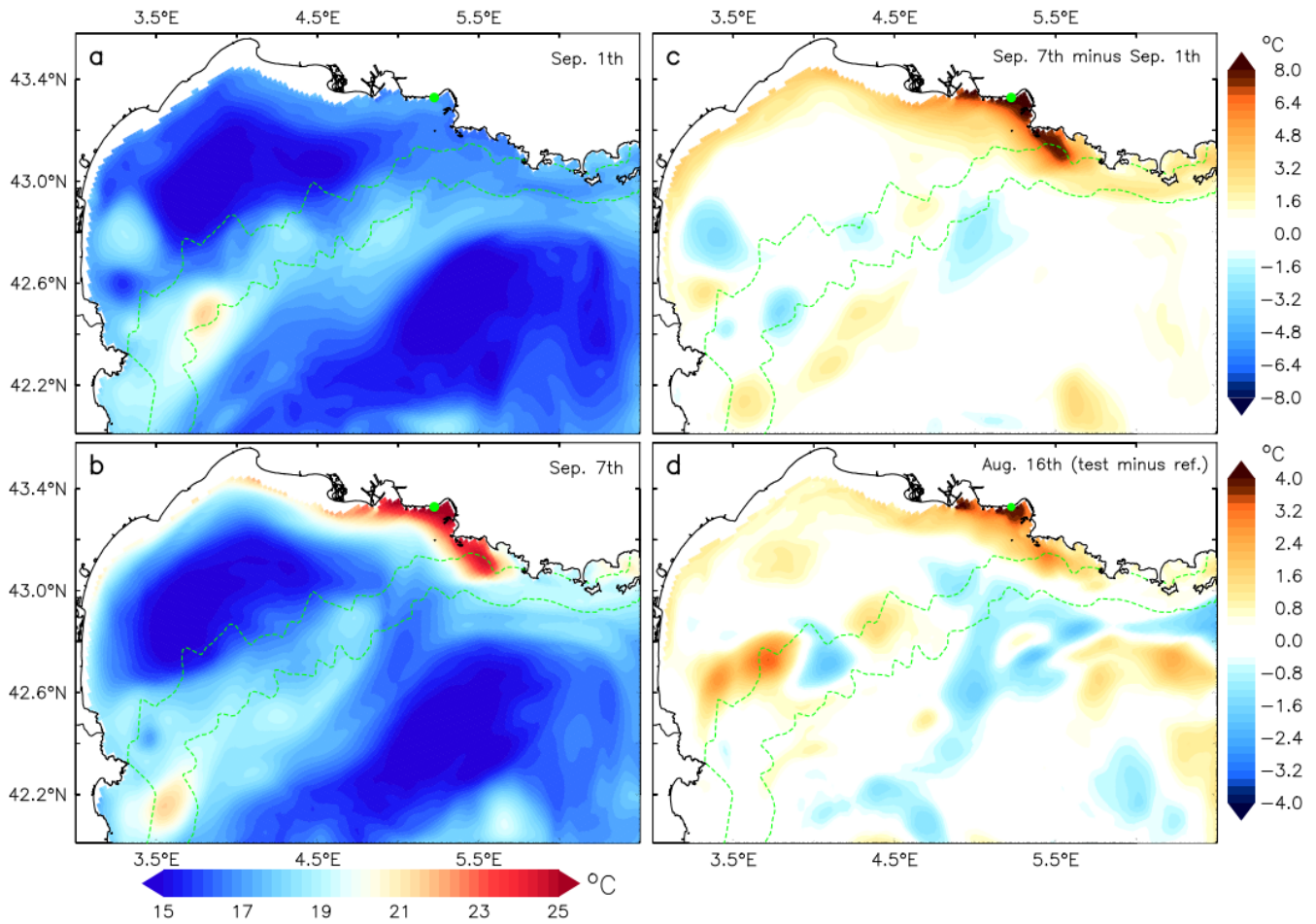


**Figure 6: (a-c): September event. Temperature (°C) at 30 m depth before the September subsurface warming event (a : September 1) and at the peak of the event (b: September 7); (c) warming between these two dates; (d) August event. Temperature difference (°C) at 30 m depth on August 16 between the test (extension of the southeasterly wind period) and the reference simulations. The green dashed lines are the 200 and 1000 m isobaths.**

### 4.3.3 Sensitivity of heat penetration in depth to the duration of the southeasterly wind

We consider the mid-August event at Méjean, the warmest of the summer at the surface. We described it as a succession of two main events (Fig. 2e-f) : one with weak winds from August 8 to 12, and the second with sustained southeasterly winds from August 12 to 14 (Fig. 4a), when sponge mortality in the Bay of Marseille began to be observed. This mortality was massively concentrated in the 0-25 m layer and more sparsely at 30 m. The second event is not detailed because it is similar to the one in September, except that, as mentioned in the previous paragraph, the duration of the southeasterly wind was shorter and the deep warming was lower in August. To understand the relation between warming and the duration of the southeasterly wind, we conducted a sensitivity study to this duration. The sustained wind event lasted about 40 hours. As the occurrence of southeasterly winds is high in August 2022 (fig. A2), we limit ourselves to extension of the

~~southeasterly wind period by one day. Knowing that the occurrence of southeasterly winds is rare in summer and that August 2022 was well above average for this occurrence (Fig. A2), we limited ourselves, to remain realistic, to extend the southeasterly wind by one day.~~ This modification was made during the weakening wind period from 1 PM on August 14 to 1 PM on August 15, where we substituted the stronger wind from the period of 1 AM on August 13 to 1 AM on August 14. The temperature at 30 m of the reference simulation being underestimated from August 15 to 18 by 3 °C on average (Fig. 2), we will subsequently present differences between the test and the reference simulations rather than the biased warming for each simulation. Figure 6d represents this temperature difference at 30 m on August 16. As expected, the lengthening of the ~~period of southeasterly winds period~~ results in increased warming. The temperature difference at 30 m from August 15 to 17 exceeds 3.5 °C around Marseille. The daily average temperature observed on August 14 and 15 was 23.8 °C. If we transpose the results of the sensitivity test to the observed series, we deduce that the temperature at 30 m would have reached the value at 20 m. This would likely have led to a deepening of the mass mortality zone to 30 m instead of 25 m, and partial mortality at 35 m due to an increased warming of 1.3 °C compared to the reference simulation. It can be seen that the maximum warming along the Gulf of Lion coast is in the same place as in the early September situation (Fig. 6c). This is also where the southeasterly wind is strongest during the warming period (Fig. 4a).

#### 4.4 Impact on marine benthic communities

Under the influence of southeasterly wind regimes, which induced warm water downwelling to a depth of 30 m, and MHWs that exhibited heightened intensity across a 600 km<sup>2</sup> area between 5.62 °E (east of Cassis) and 4.85 °E (near the Rhône River mouth), gorgonian mortality was observed to be both more severe and extended to greater depths within this region. Generally speaking, the impact on gorgonian populations appears to be most severe in the “Cap Sicié”, “Parc National des Calanques”, and “Parc Marin de la Côte Bleue” areas, particularly for the red gorgonian (*P. clavata*). For this species, which is the most sensitive, more than 50% of the populations monitored in the 20 to 30 m depth range in the PnCal showed a severe impact (> 60% of affected colonies), compared with less than 10% in Port Cros for the same depth range (Fig. 7). More specifically, in line with the MHWs observed, no impact has been recorded for the *E. cavolini* in the PNPC area, while a sometimes severe impact has been recorded for this species in the PnCal and PMCB areas. The same observation was made for *E. singularis*, whose populations were ~~less~~ affected (10-30% affected colonies) in the PNPC area for the 10-20 m depth range and were not affected deeper, while the populations were sometimes severely affected (> 60% of affected colonies) down to 20 m in the PnCal area, and moderately affected (30-60% of affected colonies) in the PMCB down to 30 m. These observations suggest a greater impact at greater depths (down to 30m) for the gorgonian populations around the Marseille region than within the PNPC.

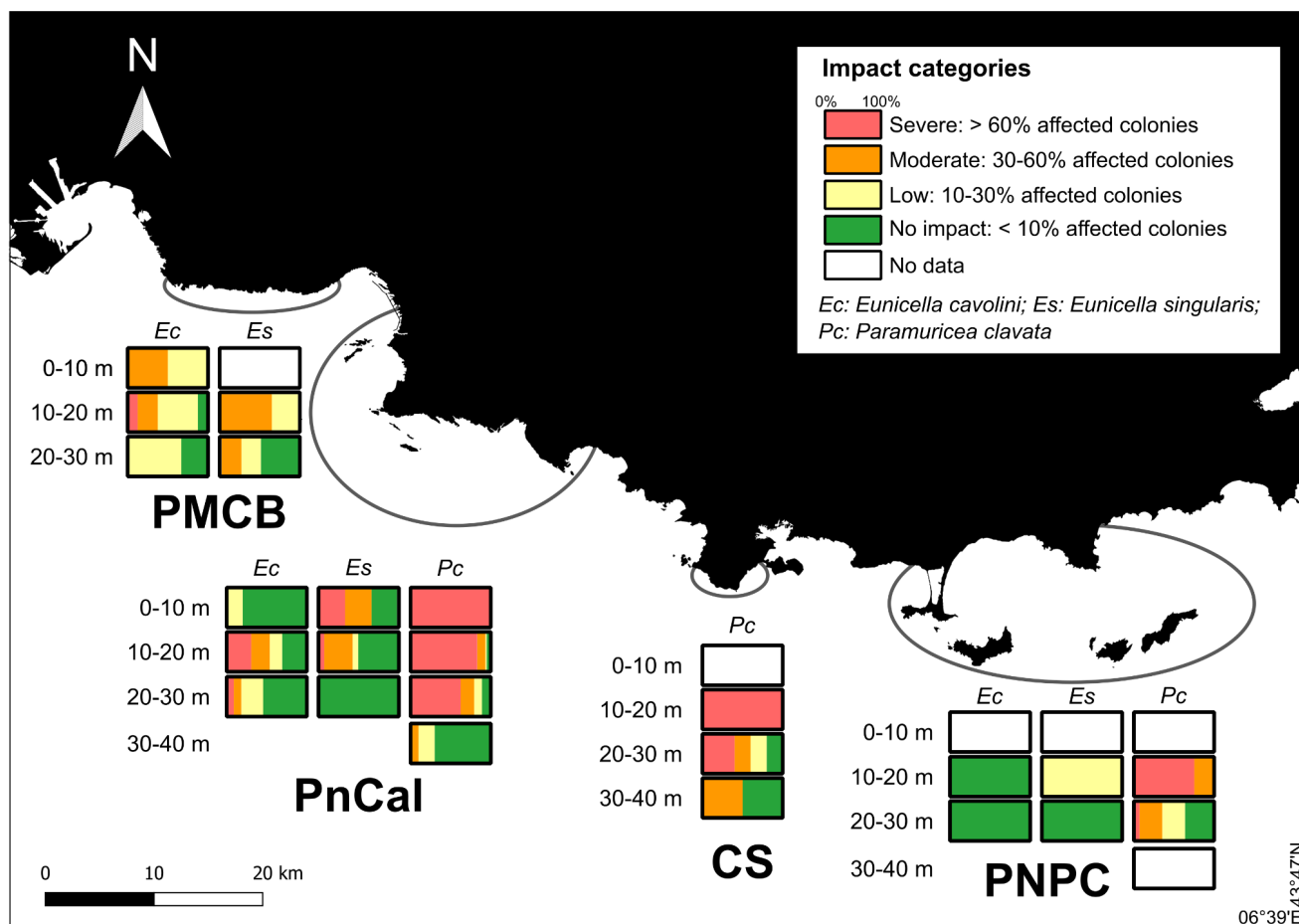


**Figure 7: Map showing the severity of the impact of the mass mortality event on the gorgonian populations of the “Parc Marin de la Côte Bleue” (PMCB), the “Parc National des Calanques” (PnCal), the “Cap Sicié” (CS), and the “Parc National de Port-Cros” (PNPC). The impact on populations is represented by 10 m depth ranges between the surface and 40 m. See Estaque et al. (2023) for more details on the monitoring method. Data for *P. clavata* in the PnCal are presented in more detail in Estaque et al. (2023).**

#### 4.5 Variability of deep heatwaves on a regional scale

Figure 3 illustrates the major spatial variability of the upper layers temperature chronology on a regional scale. The upwelling and downwelling temperature alternations discussed at Méjean are much reduced at the other two sites. Villefranche-sur-Mer is characterized by the presence of warm water throughout the summer in the surface layer, due to warming by the Northern Current flowing close to the coast and weak winds. Surface temperatures are frequently as high as the maximum recorded at Méjean on August 15. The two deep heatwave events studied at Méjean are also present at Villefranche-sur-Mer, also indicating the influence of the easterly wind in this region, albeit attenuated compared with the Marseille area (Fig. 3), which reduces the depth impacted by downwelling by about 10 m. At Banyuls-sur-Mer, the situation is different from the two other sites, with repeated temperature peaks almost reaching 40 m. The deep heatwave events of mid-August and early September studied at Mejean are also present, albeit a few days late but temperature peaks are lower

391 | than at the two other sites-, reflecting the reduced influence of the Northern Current over most of the Gulf of Lion shelf and  
392 | the frequent presence of dry northerly winds cooling the surface.

## 393 | 5. Discussion and perspectives

394 | During the summer of 2022, the atmospheric heatwaves that hit Western Europe gave rise to extreme marine heatwaves  
395 | across the western Mediterranean [as shown by Guinaldo et al. \(2023\)](#). Although being a coastal zone relatively tempered by  
396 | the recurrence of northerly winds and associated upwelling, the east of the Gulf of Lion and the very rich benthic ecosystems  
397 | that it shelters have been exposed to short periods of exceptional temperatures.

398

399 | The succession of hot and cold events in summer 2022 has been successfully reproduced by [the](#) numerical simulation: all  
400 | events have been simulated and the correlations are generally above 0.9. To go further, the precise reproduction of warm  
401 | events is a major issue when it comes to determining the crossing of thermal thresholds representing the survival of marine  
402 | species. In order to improve this precision, we identify two sensitive points here. On the one hand, a higher resolution of the  
403 | horizontal grid will improve the description of the strong bathymetric gradients characteristic of the coastal area around  
404 | Marseille and further east, along the Ligurian coast, and consequently the representation of horizontal and vertical  
405 | movements. On the other hand, the accuracy of the near-shore wind field is likely crucial for the accuracy of simulated  
406 | temperatures due to the influence of topography on wind channeling and acceleration. Exploring the uncertainties of these  
407 | two origins would be informative to improve the description of risk areas and to be able to predict extreme temperatures with  
408 | better precision without unnecessarily increasing computational costs.

409

410 | Despite the uncertainties, our modeling results provide insights [oi](#)nto the two types of heatwaves that were recorded in 2022.  
411 | The first type of heatwave is a surface phenomenon. The physical processes at play are recurrent when the northerly winds  
412 | and induced upwelling stop, and the wind speed following the northerly wind is less than  $\sim 5 \text{ m}\cdot\text{s}^{-1}$ . This succession of  
413 | meteorological conditions causes an intrusion of warm water from the Northern Current along the northeast coast of the Gulf  
414 | of Lion. In these situations, only the 5 m level exceeded 25 °C. In summary, these events renew the coastal ~~surface~~ water  
415 | mass by an advection of warm water until the following northerly gale which replaces the surface water with cold subsurface  
416 | water. The second type of heatwave, more dramatic because it affected depths of 30 to 40 m, is generated by southeasterly  
417 | winds (around  $8 - 10 \text{ m}\cdot\text{s}^{-1}$ ). Surface heating is still due to the advection of warm water from the east but it is pushed  
418 | downward by wind-induced coastal downwelling. The strength and duration of the southeasterly wind are crucial parameters  
419 | which determine the depth impacted. [This second type of events marked by pronounced sub-surface heatwaves induced by  
420 | downwelling was highlighted by Juza et al. \(2022\) and Darmaraki et al. \(2024\) in other Mediterranean regions.](#)

421



On a regional scale (~ 200 km), we have shown considerable variability in surface and deep heatwaves for two reasons: (i) the channeling of northerly and easterly winds by the continental relief [associated with the complex shape of the coastline](#), which produces localized upwelling and downwelling, and (ii) warming by the Northern Current, whose influence is great along the Ligurian coast and reduced in the western part of the Gulf of Lion. [This high spatio-temporal variability of heatwaves in coastal areas contrasts with heatwaves in open seas, which are much more widespread and also more spatially homogeneous.](#) TMED-Net network is an extremely valuable tool for documenting this variability and providing a database for validating high-resolution numerical models-.

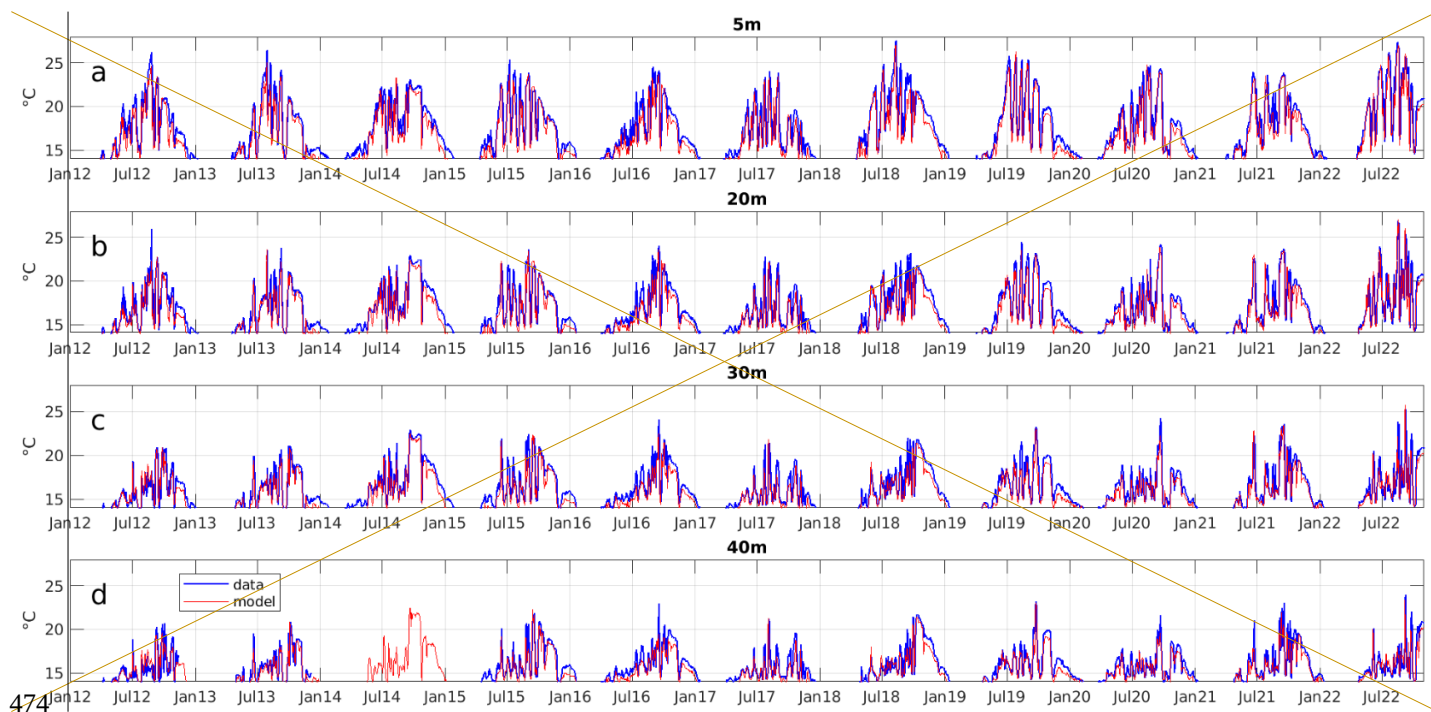
The severity of the 2022 summer for benthic species is the result of the superposition of two conditions, both exceptional, which are (1) the atmospheric heatwave which led to an exceptional warming of the surface of the western Mediterranean [Sea](#) and (2) the two southeasterly wind events in mid-August and early September which caused these warm waters to plunge to depth. These [latter](#) events are rare in summer as evidenced by the monthly downwelling index which is the highest in the decade for August, to which must be added the major event that occurs at the beginning of September. The occurrence of sustained southeasterly winds in summer, when surface temperatures are warmest, therefore constitutes a major danger for coastal ecosystems particularly for benthic species located above 40 m depth. ~~Unfortunately,~~ the coastal region around 30 km on either side of Marseille, with its remarkable habitats, is at far greater risk than the rest of the Gulf of Lion, due to the acceleration of southeasterly winds caused by the topography, which locally intensifies downwelling. Indeed, we have verified that the acceleration shown here for the two major events of August and September [2022](#) exists in most of southeasterly wind situations occurring between June and September [over the period 2012-2022](#). This is indirectly confirmed by Odic et al (2022) who, using the wind from the ERA5 reanalysis to calculate upwelling and downwelling indices, showed that the Marseille vicinity is not only the most powerful upwelling zone in the northern Gulf of Lion, but also the most exposed to downwelling.

Global warming was proven to have contributed to the extreme temperatures experienced in the western Mediterranean [Sea](#) during the summer of 2022 ([Faranda et al., 2023](#)). Exploring the coincidence of southeasterly winds and surface heatwaves in future climate scenarios would help anticipate the recurrence of massive mortality events and ultimately the disappearance of benthic populations, which are emblematic of the Calanques region of Marseille and of the Côte Bleue. Given the ongoing global warming trends, an increase in the frequency and intensity of MHWs in the affected depth zones (0 - 30 m) and deeper is expected. These extreme thermal events are likely to severely impact the potential recovery of benthic organism populations, and the potential role of refuge from deeper populations is not certain (Bramanti et al., 2023). Certain benthic species, such as gorgonians, play a crucial role as ecosystem engineers, contributing significantly to habitat complexity (Verdura et al., 2019). The collapse of these species would therefore lead to a marked reduction in structural diversity, with cascading effects on the broader ecosystem, including the disruption of ecological functions (Ponti et al., 2014) and the loss of vital ecosystem services (Estaque et al., 2023; Garrabou et al., 2021; Gómez-Gras et al., 2021). To mitigate these impacts,

456 it is imperative to adopt multidisciplinary approaches that integrate ecological, oceanographic, and climatological data to  
457 better predict the occurrence and intensity of MHWs. Such strategies are essential for developing adaptive coastal area  
458 management and conservation efforts, with the goal of preserving the integrity of Mediterranean benthic communities and  
459 maintaining the ecosystem services they provide. In a context where management plans are predominantly designed within a  
460 two-dimensional framework (Jacquemond et al., 2024), this approach marks a critical advancement towards recognizing the  
461 ocean as a three-dimensional environment, particularly when establishing marine protected areas and conservation zones.  
462  
463 Finally, heatwaves will not only intensify in frequency and intensity with climate change but thermal stress will combine  
464 with other stresses whether linked to the long-term increase in anthropogenic CO<sub>2</sub> or to the short-term impact of heatwaves  
465 on the chemical and biogeochemical composition of water. An extension of this study towards the impact of the 2022  
466 heatwaves on oxygen, [pH](#) and chlorophyll concentrations in the Gulf of Lion is planned.  
467

Surface event	5 m <b>heatwarming</b>	20 m <b>heatwarming</b>	30 m <b>heatwarming</b>	40 m <b>heatwarming</b>
June 13-18	4.8	4.2	2.3	1.8
July 9-12	6.7	5.4	2.6	1.4
August 1-4	4.1	4.7	3.6	2.
August 8-12	4.7	4.2	2.	1.1
August 23-25	6.8	6.4	4.8	3.
<b>Average</b>	<b>5.4</b>	<b>5.</b>	<b>3.</b>	<b>1.9</b>
Subsurface event	5 m <b>heatwarming</b>	20 m <b>heatwarming</b>	30 m <b>heatwarming</b>	40 m <b>heatwarming</b>
August 12-14	0.6	5.6	5.8	1.9
September 2-7	2.1	7.5	8.8	8.5
<b>Average</b>	<b>1.4</b>	<b>6.5</b>	<b>7.3</b>	<b>5.2</b>

**Table A1: Identification of the different surface and subsurface warm events. Warming in °C observed at Méjean over each period at different depths (TMED-Net data).**



474



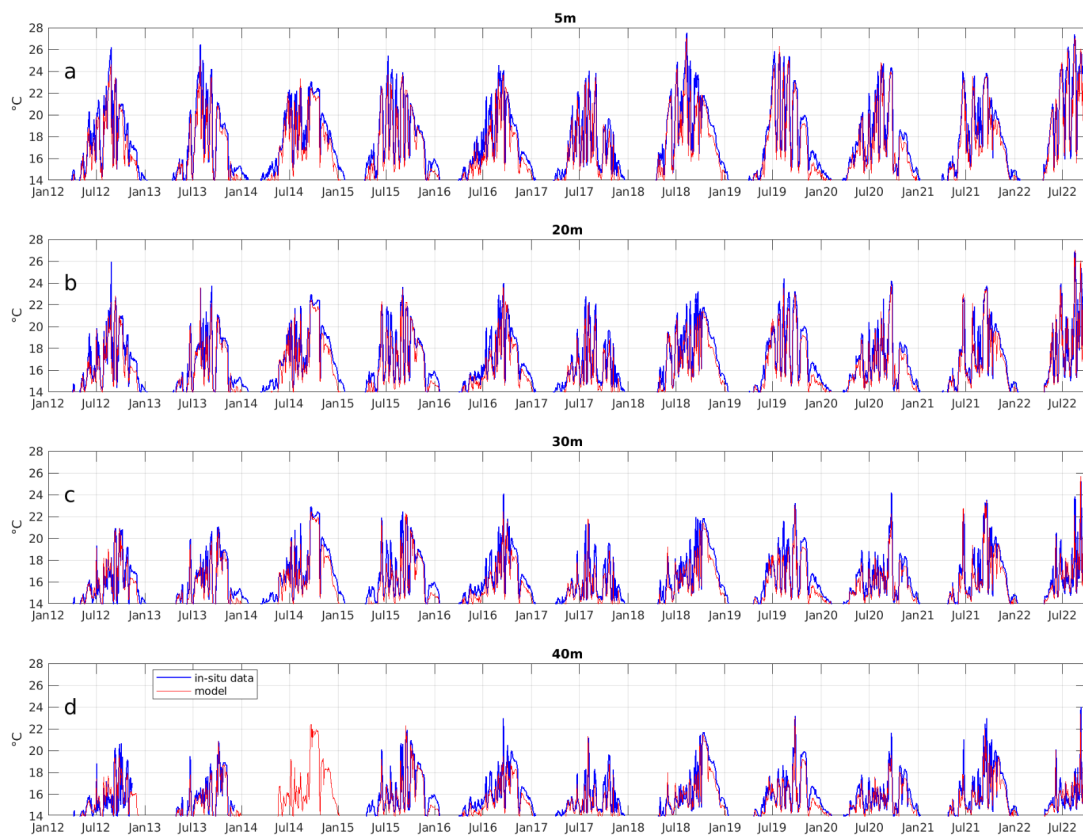
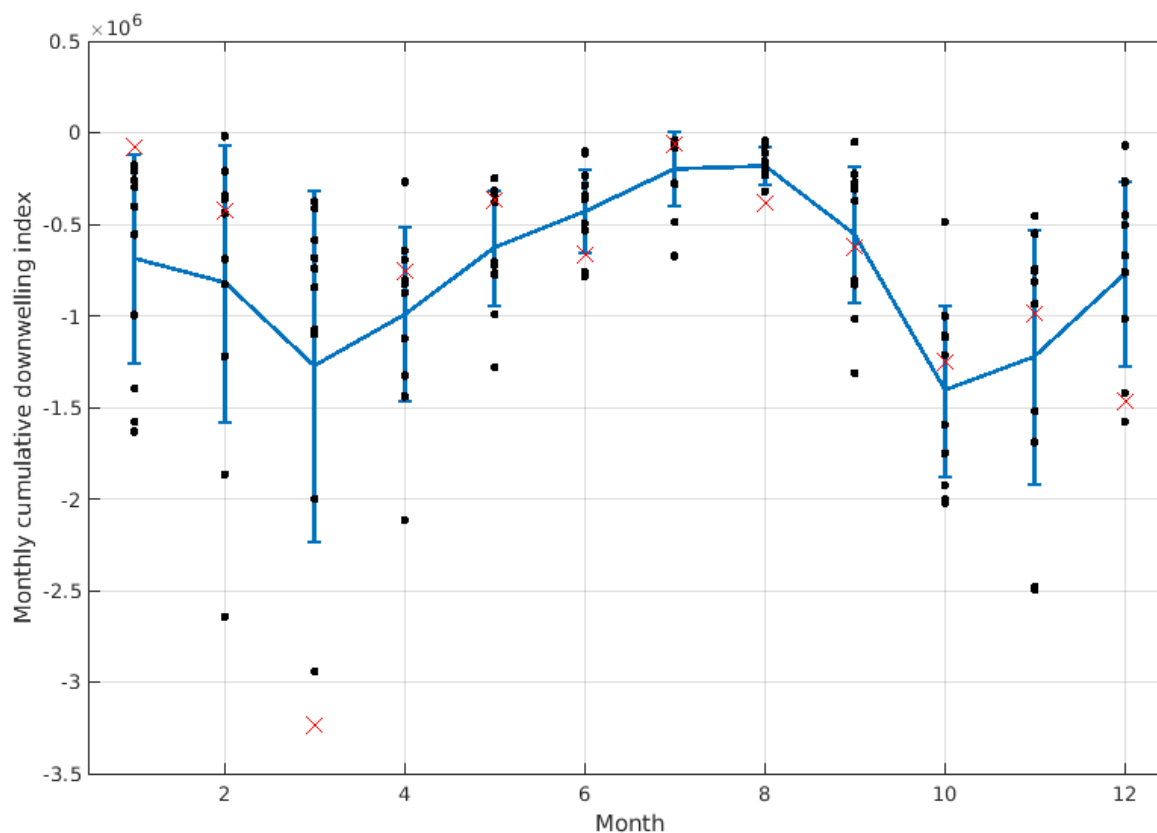


**Figure A1: Observed (blue) and simulated (red) temperature time series at the Méjean stationpoint of the TMED-Net network from 2012 to 2022 from 5 m to 40 m as indicated above the figures. The frequency shown is daily. Note the absence of in-situ data in 2014 at 40 m due to technical problems.**



479

480 | **Figure A2: Monthly cumulative downwelling index ( $\text{m}^3 \cdot (\text{coastline m})^{-1}$ ) off Marseille. Blue curve: climatology  $\pm$  standard deviation calculated over 2012-2022. Black dots represent the monthly values for each year and the red cross is for 2022.**

481

## 482 Author contribution

483 CU and CE planned the study and conceptualized the paper. TE analysed the biological data. The model was developed by  
 484 PM. CE and PM performed the simulations. QBB analysed the meteorological forcing. CE and TE wrote the first version of  
 485 the paper. All co-authors edited and corrected the text.

## 486 Competing interests

487 The authors declare that they have no conflict of interest.

488

## 489 Acknowledgments

490 This study was funded by the OFB (Office français de la biodiversité) and ILICO littoral and coastal research infrastructure  
 491 ([www.ir-ilico.fr](http://www.ir-ilico.fr)) through the INTEGRATION workshop for the study of marine heatwaves along the French coastline. The

59  
60

temperature [in-situ](#) data have been provided by the regional temperature observation network T-MEDNet, [www.t-mednet.org](http://www.t-mednet.org), site "Méjean", Dorian Guillemain, OSU Institut Pythéas, site "Villefranche-sur-Mer", Nuria Teixido and Steeve Comeau, Laboratoire d'Océanographie de Villefranche-su-Mer, site "Banyuls-sur-Mer", Ronan Rivoal, Réserve Naturelle Marine de Cerbère Banyuls /Conseil Départemental des Pyrénées Orientales. For the health data on gorgonian populations, we would like to thank Eric Charbonnel, Patrick Bonhomme, Pauline Vouriot, Stéphane Sartoretto, Quentin Schull, Bastien Mérigot and the entire Septentrion Environnement team. The SYMPHONIE model and the simulations produced are distributed by the national service SIROCCO (<https://sirocco.obs-mip.fr>) of CNRS-INSU coordinated by the ILICO research infrastructure. –The simulations were performed using HPC resources from CALMIP (Grant P09115). CE is grateful to Pierre Chevaldonné and Thierry Perez for their constructive feedback.

## References

- [Barrier, N., Petrenko, A.A., and Ourmières, Y.: Strong intrusions of the Northern Mediterranean Current on the eastern Gulf of Lion: insights from in-situ observations and high resolution numerical modelling. \*Ocean Dynamics\* 66, 313–327, 2016. doi:10.1007/s10236-016-0921-7](#)
- Bensoussan, N., Romano, J. C., Harmelin, J. G., and Garrabou, J.: High resolution characterization of Northwest Mediterranean coastal waters thermal regimes: To better understand responses of benthic communities to climate change. *Estuarine Coastal Shelf Science*, 87, 431–441. doi:10.1016/j.ecss.2010.01.008, 2010.
- Bramanti, L., Manea, E., Giordano, B., Estaque, T., Bianchimani, O., Richaume, J., Mérigot, B., Schull, Q., Sartoretto, S., Garrabou, J. G., & Guizien, K.: The deep vault: a temporary refuge for temperate gorgonian forests facing marine heat waves. *Mediterranean Marine Science*, 24(3), 601–609, doi:10.12681/mms.35564, 2023.
- Crisci, C., Bensoussan, N., Romano, J.-C., and Garrabou, J.: Temperature anomalies and mortality events in marine communities: Insights on factors behind differential mortality impacts in the NW Mediterranean. *PLoS One*, 6(9), e23814, doi:10.1371/journal.pone.0023814, 2011.
- Damien, P., Bosse, A., Testor, P., Marsaleix, P., Estournel, C.: Modeling post-convective submesoscale coherent vortices in the northwestern Mediterranean Sea. *J. Geophys. Res. Oceans*, doi:10.1002/2016JC012114, 2017.
- [Darmaraki, S., Denaxa, D., Theodorou, I., Livanou, E., Rigatou, D., Raitzos E.D., Stavrakidis-Zachou, O., Dimarchopoulou D., Bonino, G., McAdam, R., Organelli, E., Pitsouni, A., & Parasyris, A. \(2024\). Marine Heatwaves in the Mediterranean Sea: A Literature Review. \*Mediterranean Marine Science\*, 25\(3\), 586–620. <https://doi.org/10.12681/mms.38392>](#)
- Drobinski, P., and Coauthors: HyMeX: A 10-Year Multidisciplinary Program on the Mediterranean Water Cycle. *Bull. Amer. Meteor. Soc.*, 95, 1063–1082, doi:10.1175/BAMS-D-12-00242.1, 2014.
- Ducrocq, V., and Coauthors: HyMeX-SOP1: The Field Campaign Dedicated to Heavy Precipitation and Flash Flooding in the Northwestern Mediterranean. *Bull. Amer. Meteor. Soc.*, 95, 1083–1100, doi: 10.1175/BAMS-D-12-00244.1, 2014.

523 Estaque, T., Richaume, J., Bianchimani, O., et al.: Marine heatwaves on the rise: One of the strongest ever observed mass  
 524 mortality event in temperate gorgonians. *Global Change Biology*. 29(22):6159-6162, doi:10.1111/gcb.16931, 2023.  
 525 Estournel, C., Testor, P., Damien, P., D’Ortenzio, F., Marsaleix, P., Conan, P., Kessouri, F., Durrieu de Madron, X.,  
 526 Coppola, L., Lellouche, J.M., Belamari, S., Mortier, L., Ulses, C., Bouin, M.N., Prieur, L. : High resolution modeling of  
 527 dense water formation in the north-western Mediterranean during winter 2012–2013: Processes and budget. *Journal of*  
 528 *Geophysical Research – Oceans*, doi:10.1002/2016JC011935, 2016.  
 529 Estournel, C., Marsaleix, P. and Ulses, C.: A new assessment of the circulation of Atlantic and Intermediate Waters in the  
 530 Eastern Mediterranean. *Progress in Oceanography*, 198, 102673, doi:10.1016/j.pocean.2021.102673, 2021.  
 531 Faranda, D., Pascale, S., Bulut, B.: Persistent anticyclonic conditions and climate change exacerbated the exceptional 2022  
 532 European-Mediterranean drought. *Environ. Res. Lett.*, 18 034030, doi:10.1088/1748-9326/acbc37, 2023.  
 533 Fox-Kemper, B., H.T. Hewitt, C. Xiao, G. Aðalgeirsdóttir, S.S. Drijfhout, T.L. Edwards, N.R. Golledge, M. Hemer, R.E.  
 534 Kopp, G. Krinner, A. Mix, D. Notz, S. Nowicki, I.S. Nurhati, L. Ruiz, J.-B. Sallée, A.B.A. Slangen, and Y. Yu: Ocean,  
 535 Cryosphere and Sea Level Change. In *Climate Change 2021: The Physical Science Basis. Contribution of Working Group I*  
 536 *to the Sixth Assessment Report of the Intergovernmental Panel on Climate Change* [Masson-Delmotte, V., P. Zhai, A. Pirani,  
 537 S.L. Connors, C. Péan, S. Berger, N. Caud, Y. Chen, L. Goldfarb, M.I. Gomis, M. Huang, K. Leitzell, E. Lonnoy, J.B.R.  
 538 Matthews, T.K. Maycock, T. Waterfield, O. Yelekçi, R. Yu, and B. Zhou (eds.)]. Cambridge University Press, Cambridge,  
 539 United Kingdom and New York, NY, USA, pp. 1211–1362, doi:10.1017/9781009157896.011, 2021.  
 540 Garrabou, J., Ledoux, J.B., Bensoussan, N., Gómez-Gras, D., Linares, C.: Sliding Toward the Collapse of Mediterranean  
 541 Coastal Marine Rocky Ecosystems. In: Canadell, J.G., Jackson, R.B. (eds) *Ecosystem Collapse and Climate Change*.  
 542 *Ecological Studies*, vol 241. Springer, Cham., doi:10.1007/978-3-030-71330-0\_11, 2021.  
 543 Garrabou, J., Gómez-Gras, D., Medrano, A., Cerrano, C., Ponti, M., Schlegel, R., Bensoussan, N., Turicchia, E., Sini, M.,  
 544 Gerovasileiou, V., Teixido, N., Mirasole, A., Tamburello, L., Cebrian, E., Rilov, G., Ledoux, J.-B., Souissi, J. B., Khamassi,  
 545 F., Ghanem, R. ... Harmelin, J.-G.: Marine heatwaves drive recurrent mass mortalities in the Mediterranean Sea. *Global*  
 546 *Change Biology*, 28, 5708–5725, doi:10.1111/gcb.16301, 2022.  
 547 Gómez-Gras D., Linares C., López-Sanz A., Amate R., Ledoux J. B., Bensoussan N., Drap P., Bianchimani O., Marschal C.,  
 548 Torrents O., Zuberer F., Cebrian E., Teixido N., Zabala M., Kipson S., Kersting D. K., Montero-Serra I., Pagès-Escalà M.,  
 549 Medrano A., Frleta-Valić M., Dimarchopoulou D., López-Sendino P. and Garrabou J.: Population collapse of habitat-  
 550 forming species in the Mediterranean: a long-term study of gorgonian populations affected by recurrent marine heatwaves.  
 551 *Proc. R. Soc. B.*, 28820212384, doi:10.1098/rspb.2021.2384, 2021.  
 552 Grenier, M., Idan, T., Chevaldonné, P., Perez, T.: Mediterranean marine keystone species on the brink of extinction. *Glob.*  
 553 *Change Biol.*, 29, 1681-1683, doi:10.1111/gcb.16597, 2023.  
 554 Guinaldo, T., Voldoire, A., Waldman, R., Saux Picart, S., and Roquet, H.: Response of the sea surface temperature to  
 555 heatwaves during the France 2022 meteorological summer. *Ocean Sci.*, 19, 629–647, doi:10.5194/os-19-629-2023, 2023.

556 Glynn, P.W., D'Croz, L. : Experimental evidence for high temperature stress as the cause of El Niño coincident coral  
557 mortality. *Coral Reefs*, 8, 181-191, doi:10.1007/BF00265009, 1990.

558 Hughes, T., Kerry, J., Álvarez-Noriega, M. et al.: Global warming and recurrent mass bleaching of corals. *Nature*, 543, 373–  
559 377, doi:10.1038/nature21707, 2017.

560 Jacquemont, J., Loiseau, C., Tornabene, L. et al.: 3D ocean assessments reveal that fisheries reach deep but marine  
561 protection remains shallow. *Nat. Commun.*, 15, 4027, doi:10.1038/s41467-024-47975-1, 2024.

562 Juza, M, Fernández-Mora, À, Tintoré, J.: Sub-Regional Marine Heat Waves in the Mediterranean Sea From Observations:  
563 Long-Term Surface Changes, Sub-Surface and Coastal Responses. *Front. Mar. Sci.*, 9:785771,  
564 doi:10.3389/fmars.2022.785771, 2022.

565 Lejeusne, C., Chevaldonné, P., • Pergent-Martini, C., • Boudouresque, C.F., • Pérez, T. : Climate change  
566 effects on a miniature ocean: the highly diverse, highly impacted Mediterranean Sea. *Trends in Ecology & Evolution*, 25, 4,  
567 250 – 260,doi: 10.1016/j.tree.2009.10.009, 2010.

568 Marsaleix, P., Auclair, F., Estournel, C.: Considerations on Open Boundary Conditions for Regional and Coastal Ocean  
569 Models. *Journal of Atmospheric and Oceanic Technology*, 23,1604-1613, doi: 10.1175/JTECH1930.1, 2006.

570 Marsaleix, P., Auclair, F., Floor, J. W., Herrmann, M. J., Estournel, C., Pairaud, I., Ulses, C.: Energy conservation issues in  
571 sigma-coordinate free-surface ocean models. *Ocean Modelling*, 20, 61-89, doi:10.1016/j.ocemod.2007.07.005,2008.

572 Martinez, J., Leonelli, F.E., Garcia-Ladona, E., Garrabou, J., Kersting, D.K., Bensoussan, N. and Pisano, A.: Evolution of  
573 marine heatwaves in warming seas: the Mediterranean Sea case study. *Front. Mar. Sci.*, 10:1193164,  
574 doi:10.3389/fmars.2023.1193164, 2023.

575 Marullo S., et al.: Record-breaking persistence of the 2022/23 marine heatwave in the Mediterranean Sea. *Environ. Res.*  
576 *Lett.* ,18, 114041, doi:10.1088/1748-9326/ad02ae, 2023.

577 Mikolajczak, G., Ulses, C., Estournel, C., Bourrin, F., Pairaud, I., Martín, J., Puig, P., Durrieu de Madron, X., Leredde, Y.,  
578 Marsaleix, P. : Impact of storms on residence times and export of coastal waters during a mild fall/winter period in the Gulf  
579 of Lion. *Continental Shelf Research*, 207, 104192, doi:10.1016/j.csr.2020.104192, 2020.

580 Millot, C.: The gulf of Lions' hydrodynamics. *Continental Shelf Research*, 10, 9-11, 885-894, 1990.

581 Obermann-Hellhund, A., Conte, D., Somot, S. et al.: Mistral and Tramontane wind systems in climate simulations from  
582 1950 to 2100. *Clim. Dyn.*, 50, 693–703, doi:10.1007/s00382-017-3635-8, 2018.

583 Odic, R., Bensoussan, N., Pinazo, C., Taupier-Letage, I., Rossi, V.: Sporadic wind-driven upwelling / downwelling and  
584 associated cooling / warming along Northwestern Mediterranean coastlines. *Continental Shelf Research*, 250, 104843,  
585 doi:10.1016/j.csr.2022.104843, 2022.

586 Pairaud, I.L., Bensoussan, N., Garreau, P. et al.: Impacts of climate change on coastal benthic ecosystems: assessing the  
587 current risk of mortality outbreaks associated with thermal stress in NW Mediterranean coastal areas. *Ocean Dynamics*, 64,  
588 103–115, doi:10.1007/s10236-013-0661-x, 2014.



589 Pastor, F., Valiente, J.A., Khodayar, S.: A Warming Mediterranean: 38 Years of Increasing Sea Surface Temperature.  
590 Remote Sens., 12, 2687, doi:10.3390/rs12172687, 2020.

591 Pastor, F. & Khodayar Pardo, S.: Marine heat waves: Characterizing a major climate impact in the Mediterranean. Science of  
592 The Total Environment, 861, 160621, doi:10.1016/j.scitotenv.2022.160621, 2023.

593 Ponti, M., Perlini R.A., Ventra V., Grech D., Abbiati M., Cerrano C.: Ecological Shifts in Mediterranean Coralligenous  
594 Assemblages Related to Gorgonian Forest Loss. PLoS ONE 9(7): e102782, doi:10.1371/journal.pone.0102782, 2014.

595 [Ross, O.N., Fraysse, M., Pinazo, C., Pairaud, I.: Impact of an intrusion by the Northern Current on the biogeochemistry in](#)  
596 [the eastern Gulf of Lion, NW Mediterranean. Estuarine, Coastal and Shelf Science, 170, 1-9, doi:10.1016/j.ecss.2015.12.022,](#)  
597 [2016.](#)

598 Sartoretto, S., Ledoux J.B., Gueret E., Guillemain D., Ravel C., Moirand L., Aurelle D.: Ecological and genomic  
599 characterization of a remarkable natural heritage: a mesophotic ‘giant’ Paramuricea clavata forest. Mar. Ecol. Prog. Ser.,  
600 728:85-101, doi:10.3354/meps14427, 2023.

601 Schaeffer, A., Sen Gupta, A. & Roughan, M.: Seasonal stratification and complex local dynamics control the sub-surface  
602 structure of marine heatwaves in Eastern Australian coastal waters. Commun Earth Environ, 4, 304, doi:10.1038/s43247-  
603 023-00966-4, 2023.

604 Simon, A., Plecha, S.M., Russo, A., Teles-Machado, A., Donat, M.G., Auger, P.-A., Trigo, R.M. : Hot and cold marine  
605 extreme events in the Mediterranean over the period 1982-2021. Front. Mar. Sci., 9:892201, doi:  
606 10.3389/fmars.2022.892201, 2022.

607 Ulses, C., Estournel, C. , Bonnin, J., Durrieu de Madron, X., Marsaleix, P. : Impact of storms and dense water cascading on  
608 shelf-slope exchanges in the Gulf of Lion (NW Mediterranean). Journal of Geophysical Research, 113, C02010, 2008.

609 Verdura, J., Linares, C., Ballesteros, E. et al.: Biodiversity loss in a Mediterranean ecosystem due to an extreme warming  
610 event unveils the role of an engineering gorgonian species. Sci. Rep., 9, 5911, doi:10.1038/s41598-019-41929-0, 2019.

611

612